



MSU
MOSCOW
STATE UNIVERSITY
RESEARCH
COMPUTING CENTER

1



2



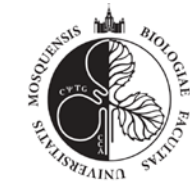
3



4



5



6



7

МОДЕЛИРОВАНИЕ ВКЛАДА ВОДНЫХ ОБЪЕКТОВ СУШИ С ГЛОБАЛЬНЫЙ УГЛЕРОДНЫЙ МЕТАНОВЫЙ ЦИКЛ

В.М. Степаненко^{1,2,3}, И.А.Репина^{4,1,3,5}

¹МГУ имени М.В. Ломоносова, Научно-исследовательский
вычислительный центр

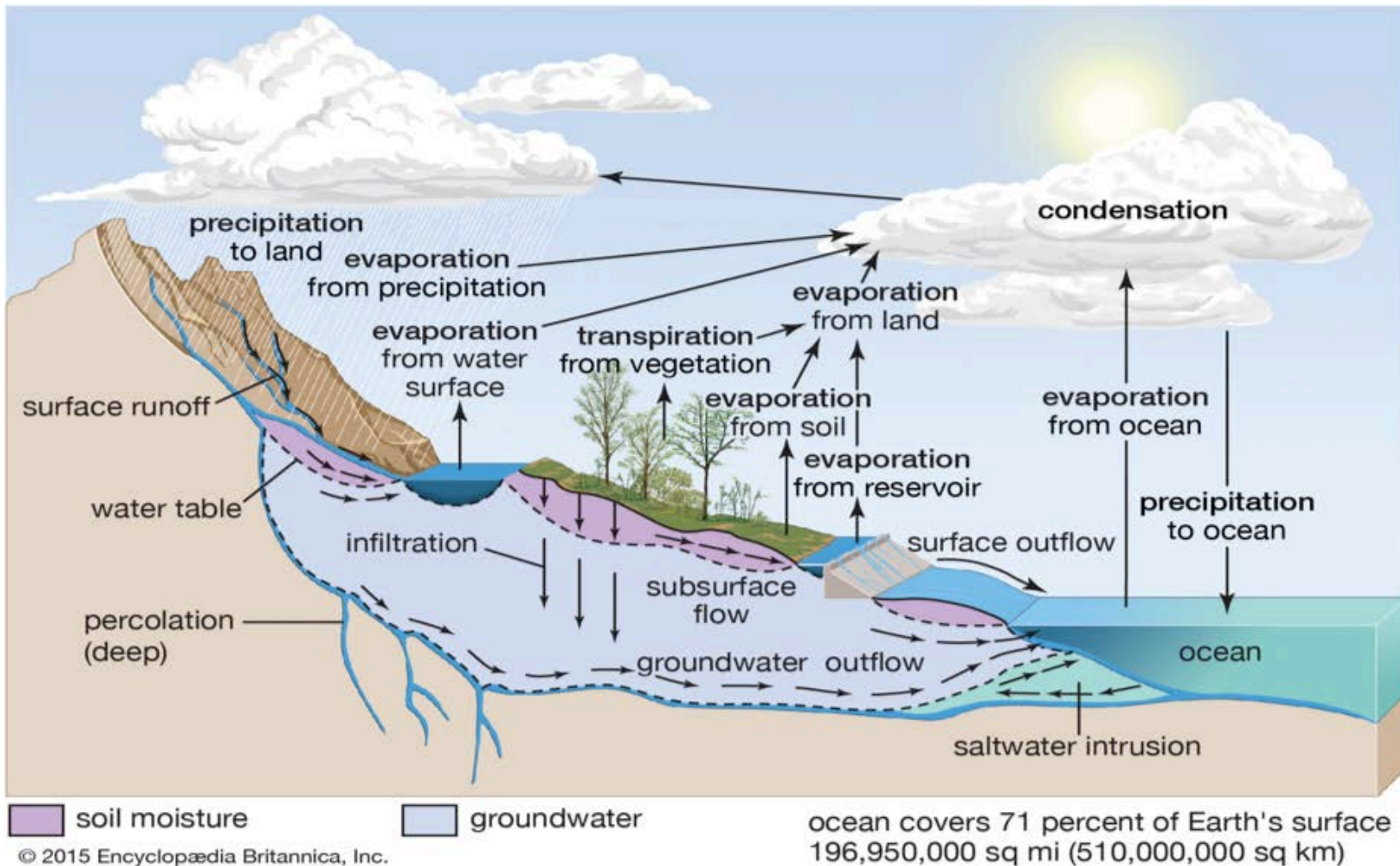
²МГУ имени М.В. Ломоносова, Географический факультет

³Московский центр фундаментальной и прикладной математики

⁴Институт физики атмосферы им. А.М.Обухова РАН

⁵Институт космических исследований РАН

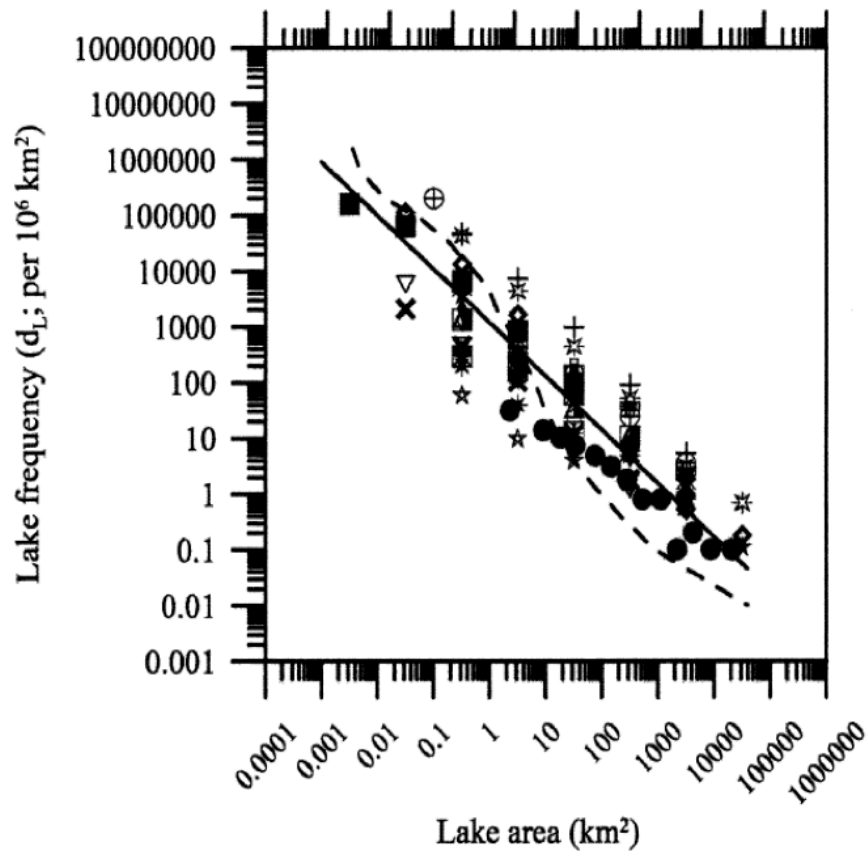
The water cycle



Water bodies occupy $\approx 1.8\%$ of land surface. Soil moisture is the key factor of surface evaporation and energy cycle. Soil moisture is the most variable component of land.



Распределение озёр по размерам (Downing et al., 2006)



Площадь озёр разных размеров (Downing et al., 2006)

Площадь озера, км^2	Суммарная площадь, км^2	пло-
0.001 – 0.01	692,600	
0.01 – 0.1	602,100	
0.1 – 1	523,400	
1 – 10	455,100	
0.001 – 10	2,273,200	
...	...	
Все озёра	4,200,000	

- Подсеточные (малые, $L < L_R$, Показеев и Филатов, 2002) водоёмы составляют **54%** площади озёр планеты
- Для крупных озёр начинают применяться трёхмерные модели в оперативном режиме
- Для подсеточных озёр одномерным моделям альтернативы нет
- Малые озёра являются основным источником парниковых газов

Vertical structure of a stratified lake

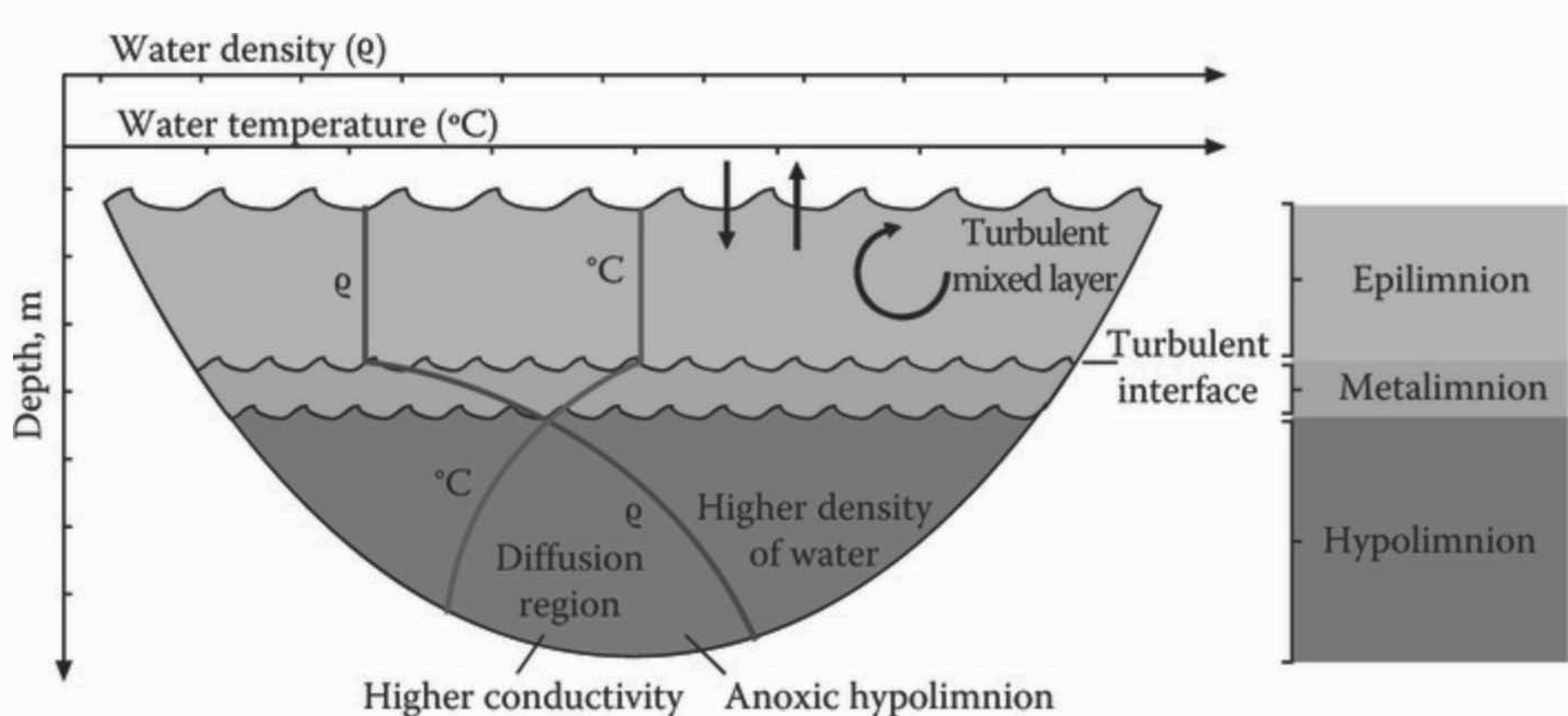
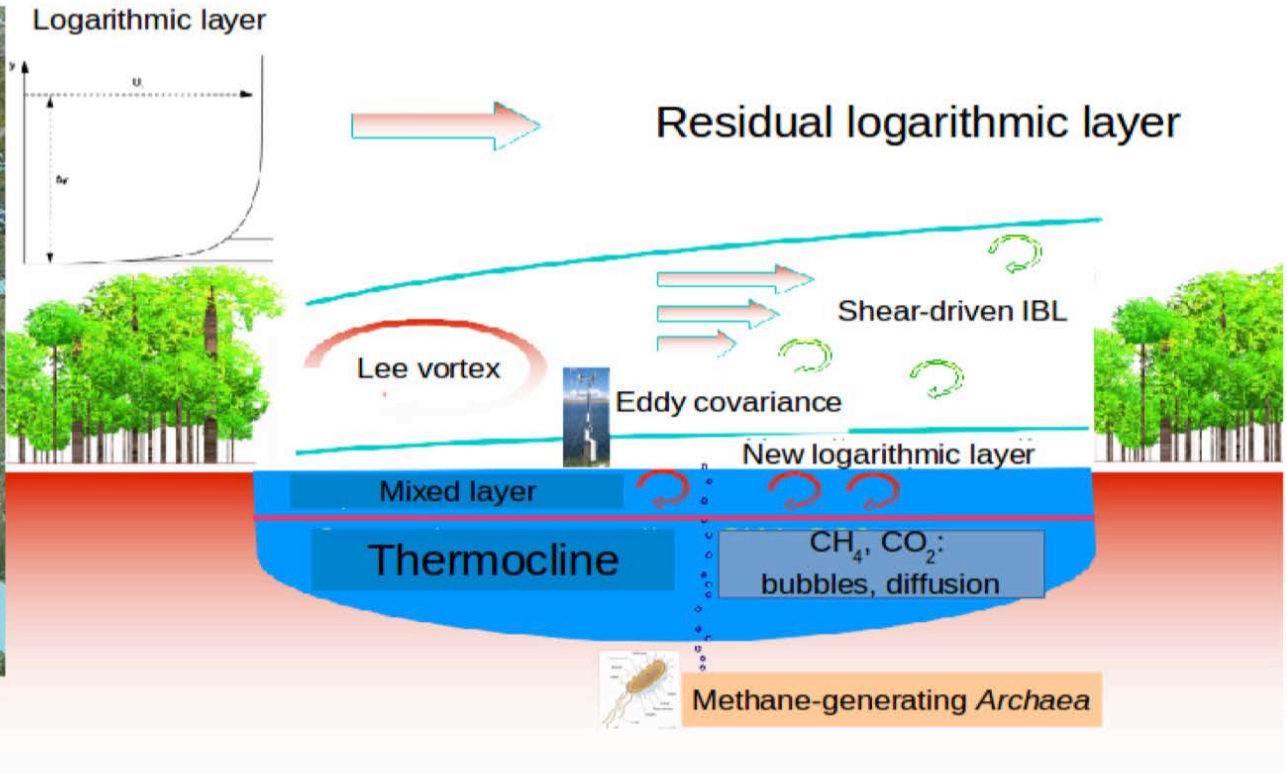


Figure 3.5 (See color insert.) Vertical structure of a stratified lake and its physical and chemical features (Original Degani and Tundisi 2011.).

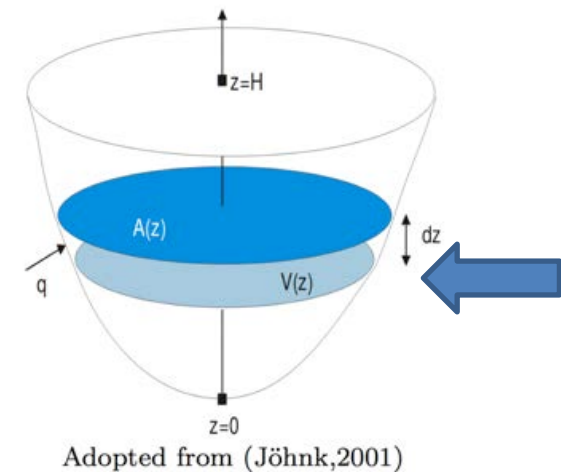
Lake-atmosphere continuum



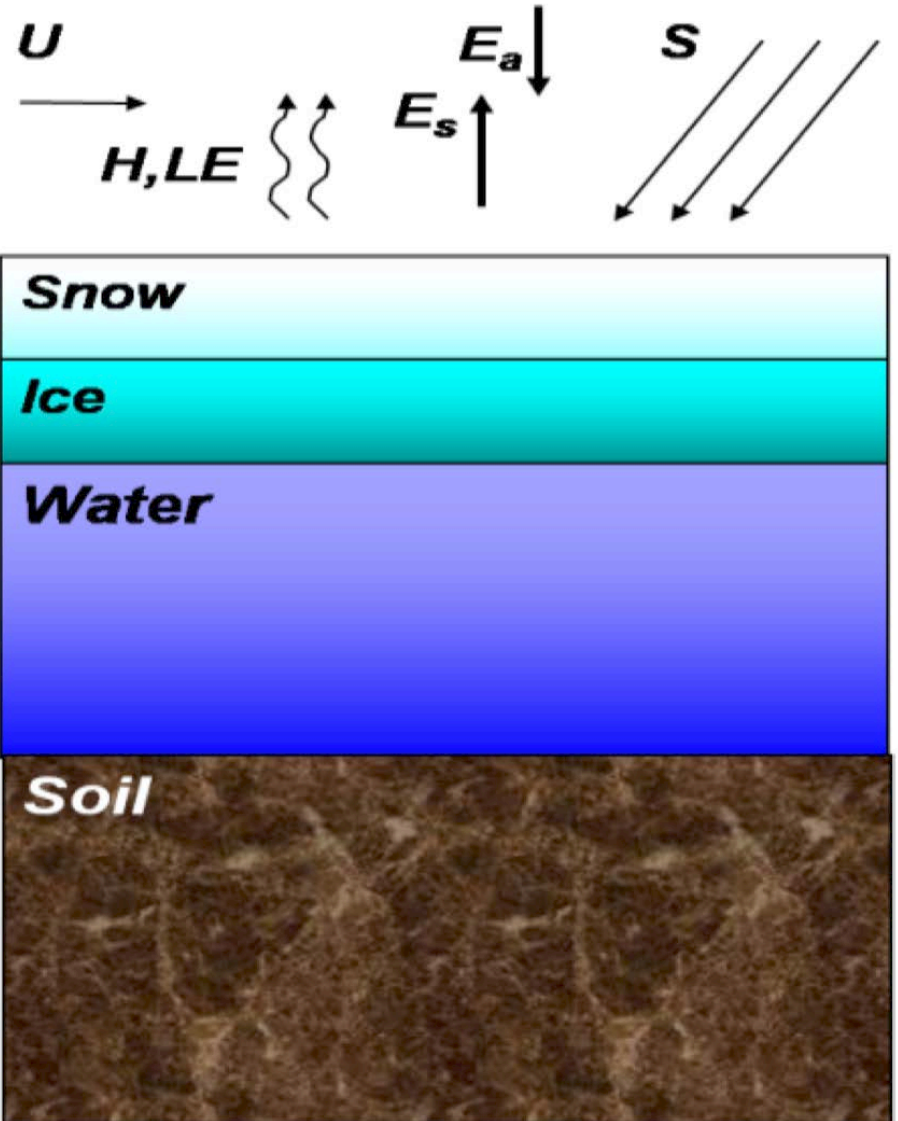
- Lakes are abundant in a number of regions, including Finland, Karelia, Siberia, Canada, China (famous for artificial reservoirs), **often surrounded by forested landscapes**
- Inland waters are currently included as **a separate tile** in many NWP and climate models, represented by 1D vertical heat transfer schemes
- **Efficient parameterizations** are needed to reproduce energy, momentum and gas exchange between “lake-forest” landscapes and the atmosphere
- **Highly-coupled problem** including in-lake and ABL processes

LAKE model: basic physics

- 1D heat and momentum equations
- $k - \epsilon$ turbulence closure
- Monin-Obukhov similarity for surface fluxes
- Beer-Lambert law for shortwave radiation attenuation
- Momentum flux partitioning between wave development and currents (Stepanenko et al., 2014)
- Soil heat and moisture transfer including phase transitions
- Multilayer snow and ice models



A general procedure of horizontal averaging allows to take into account heat and gas fluxes at the sloping bottom



LAKE model: horizontal averaging

Velocity components and scalars in incompressible fluid are governed by equations of the form:

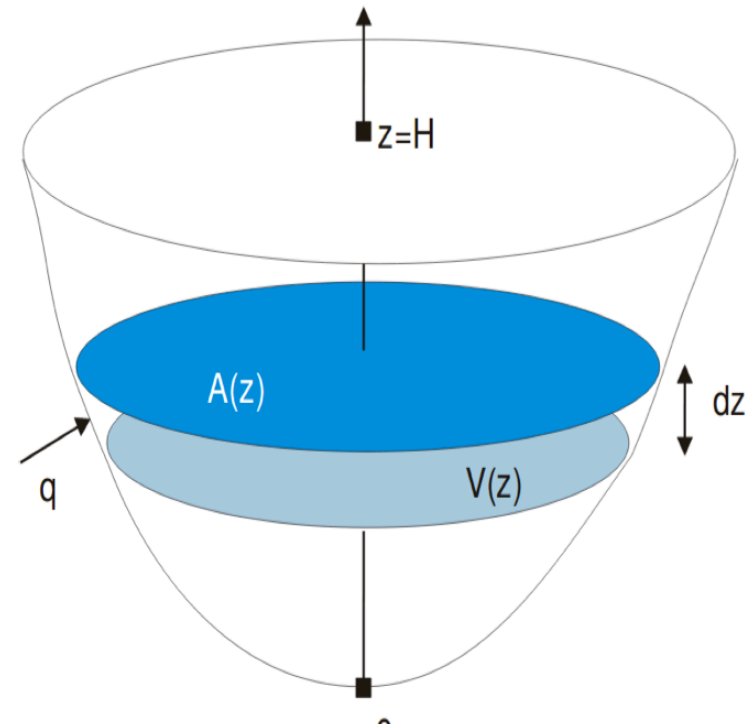
$$c \frac{\partial f}{\partial t} = -c \frac{\partial u_i f}{\partial x_i} - \frac{\partial F_i}{\partial x_i} + R_f(f, \dots),$$

Averaging over the horizontal cross-section $A(z)$:

$$\bar{f} = \frac{1}{A(z)} \int_{A(z)} f dx dy.$$

Assuming small slopes, $\bar{w} = 0$, yields:

$$c \frac{\partial \bar{f}}{\partial t} = \underbrace{-\frac{c}{A} \int_{\Gamma_{A(z)}} f (\mathbf{u}_h \cdot \mathbf{n}) dl}_{\text{Inlets and outlets}} + \underbrace{\frac{1}{A} \frac{\partial}{\partial z} \left(A k_f \frac{\partial \bar{f}}{\partial z} \right)}_{\text{Vertical diffusion}} - \underbrace{-\frac{1}{A} \frac{\partial A \bar{F}_{nz}}{\partial z}}_{\text{Div. of non-diffusion flux}} + \underbrace{\frac{1}{A} \frac{dA}{dz} [F_{nz,b}(z) + F_{tz,b}(z)]}_{\text{Bottom flux}} + \underbrace{R_f(\bar{f}, \dots)}_{\text{Sources}}.$$



Adopted from (Jöhnk, 2001)

Here, F_{tz} – vertical turbulent flux, F_{nz} – vertical non-turbulent flux of variable f .

The model of sediments

Soil heat and moisture transfer are governed by diffusion, gravity infiltration, runoff, root uptake and phase transitions:

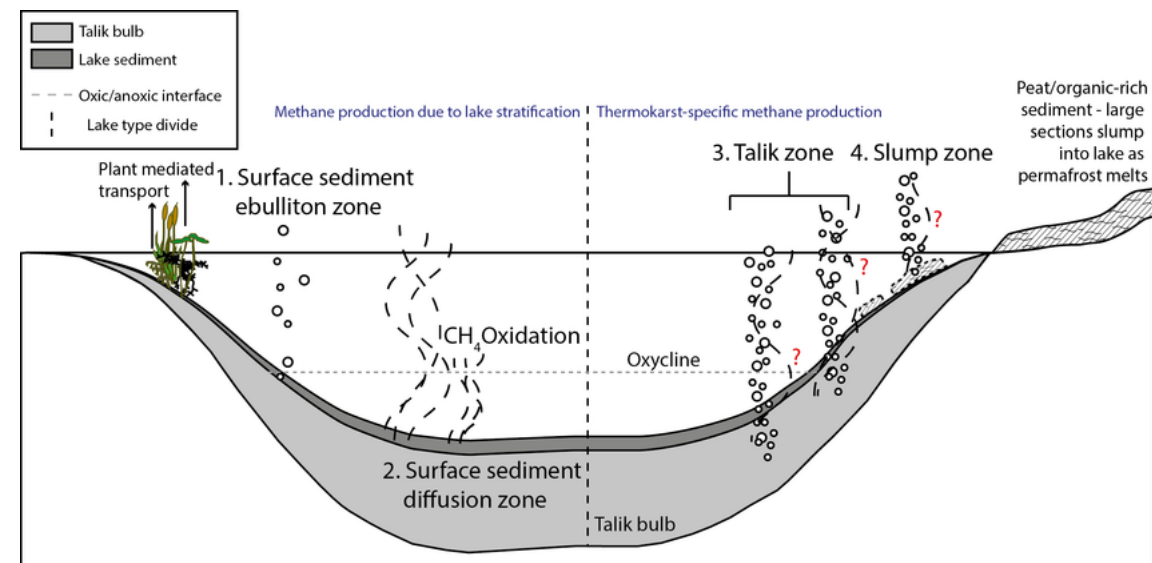
$$\rho c \frac{\partial T}{\partial t} = \frac{\partial}{\partial x} \lambda_T \frac{\partial T}{\partial z} + \rho_d (L_i F_i - L_v F_v), \textcolor{red}{T} - \text{temperature}$$

$$\frac{\partial W}{\partial t} = \frac{\partial}{\partial z} \left[\lambda_W \left(\frac{\partial W}{\partial z} + \delta \frac{\partial T}{\partial z} \right) \right] + \frac{\partial \gamma}{\partial z} - F_i - F_v - R_f - R_r, \textcolor{blue}{W} - \text{moisture}$$

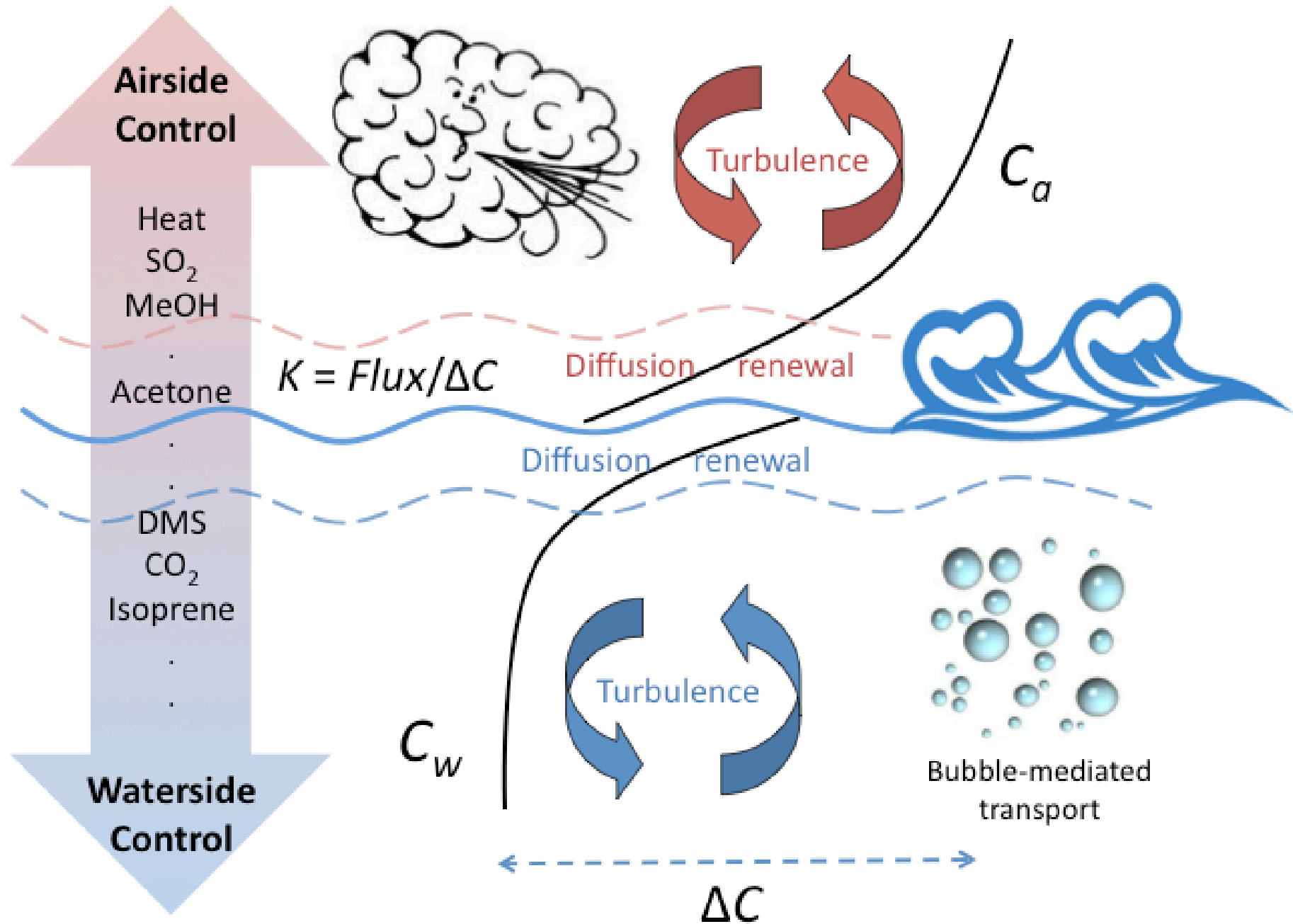
$$\frac{\partial V}{\partial t} = \frac{\partial}{\partial z} \lambda_V \frac{\partial V}{\partial z} + F_v, \textcolor{green}{V} - \text{vapour}$$

$$\frac{\partial I}{\partial t} = F_i \cdot \textcolor{brown}{I} - \text{ice}$$

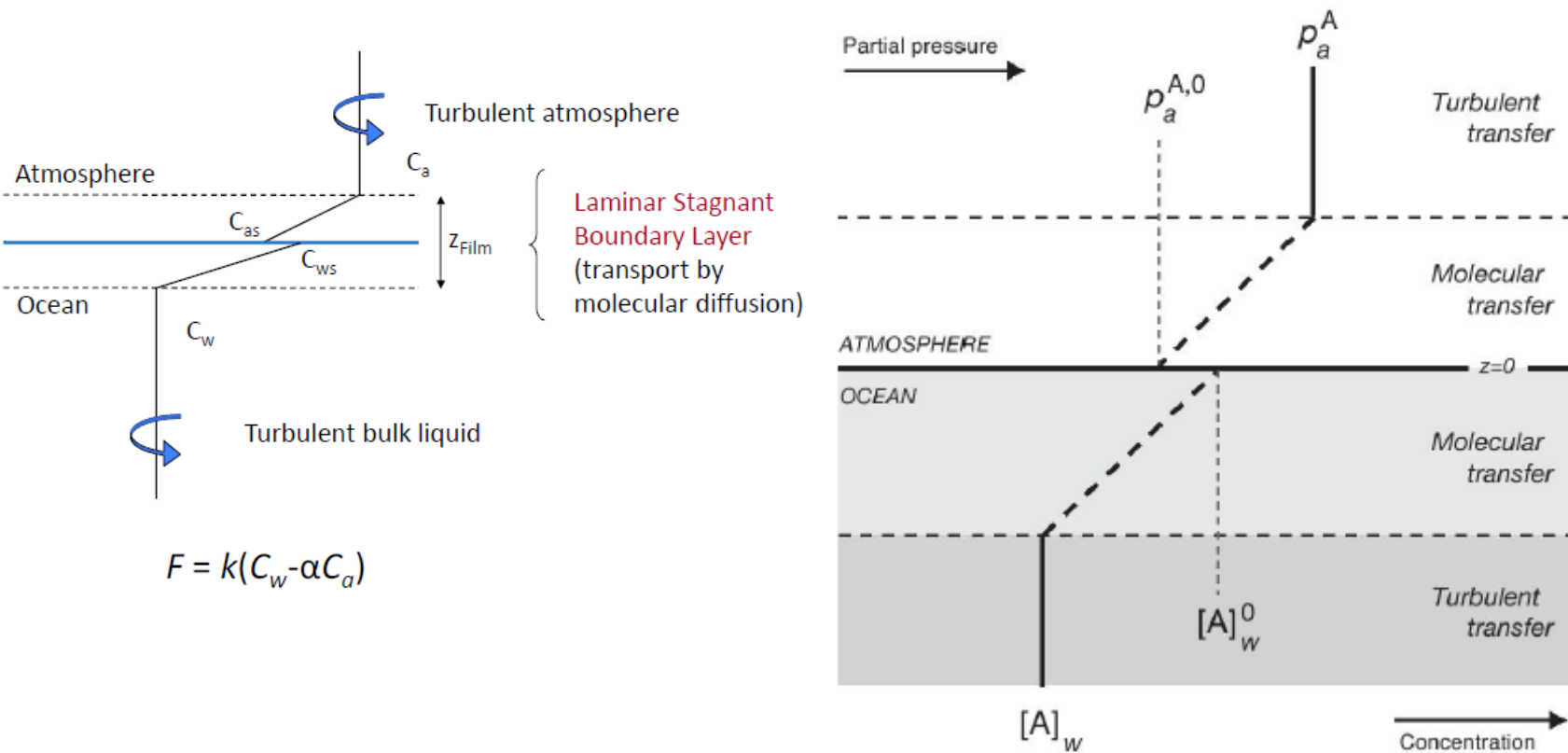
Thermal regime of sediments, including freezing/thawing is important for modeling biogeochemical processes, especially, CH₄



Механизмы переноса растворённых газов через поверхность воды



Преночный механизм газопереноса



Газы хорошо перемешаны в турбулентном слое.

Перенос происходит только через неподвижную пленку с помощью молекулярной диффузии ε .

Роль водоёмов суши в углеродном и метановом цикле

(Tranvik et al. 2009)

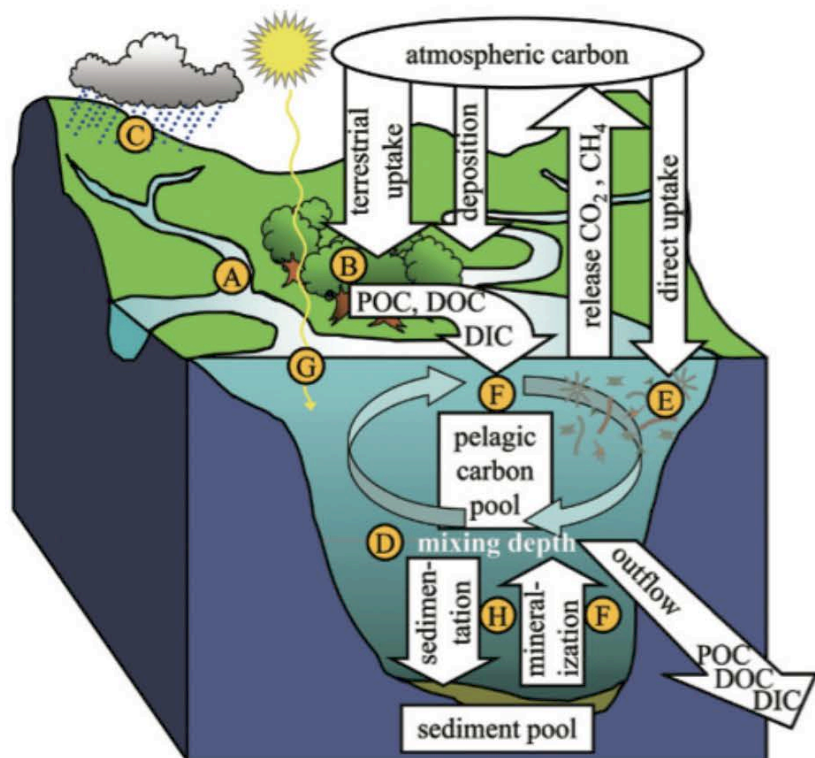


Fig. 2. Schematic diagram showing pathways of carbon cycling mediated by lakes and other continental waters. The letters correspond to rows in Table 1.

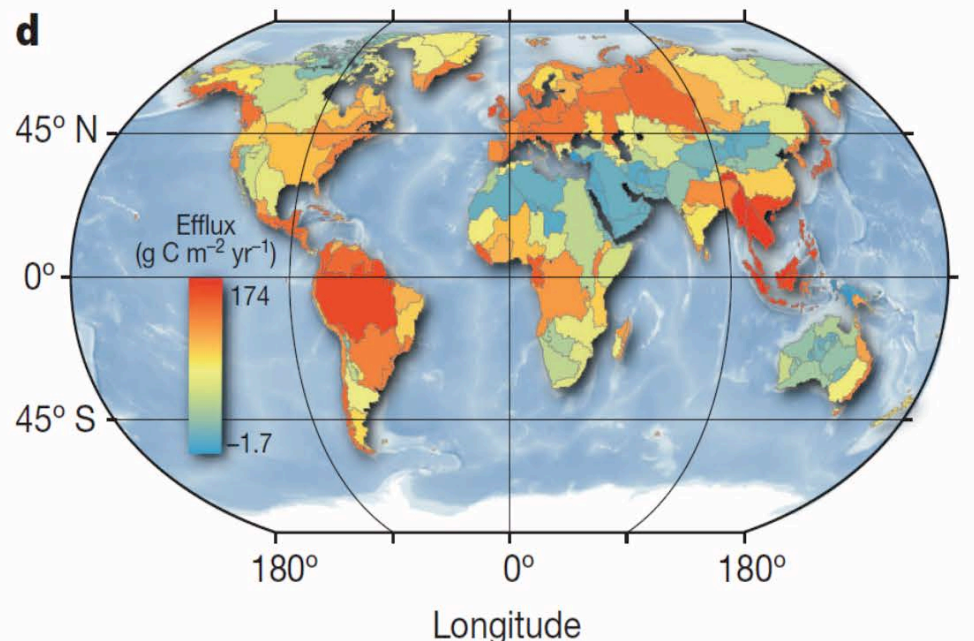
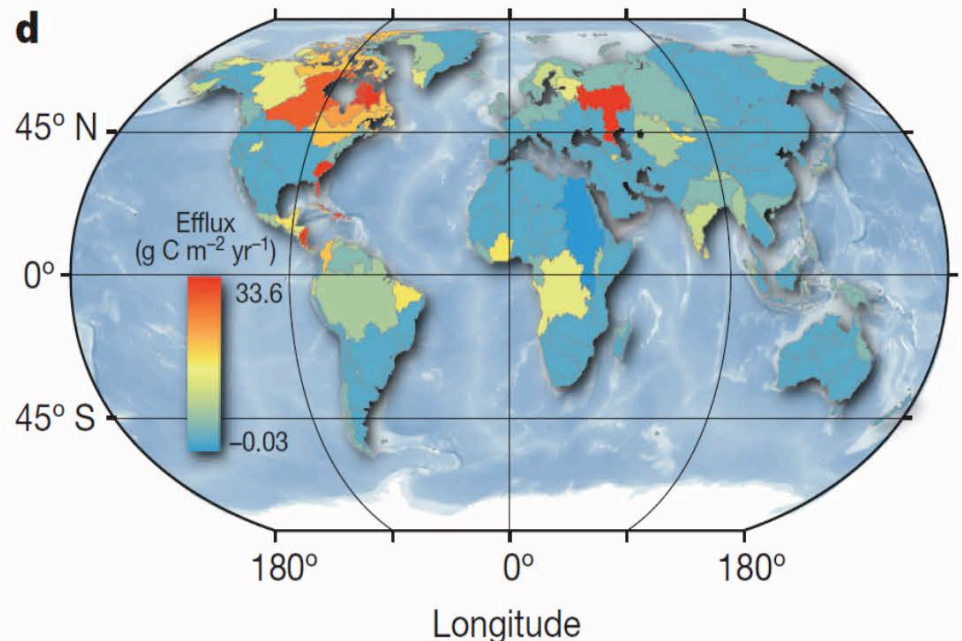
(Bastviken et al. 2011)

Latitude	Fluxes												Area (km ²)	
	Total open water			Ebullition			Diffusive			Stored				
	Emiss.	n	CV	Emiss.	n	CV	Emiss.	n	CV	Emiss.	n	CV		
<i>Lakes</i>														
>66°	6.8	17	72	6.4	17	74	0.7	60	37				288,318	
>54°–66°	6.6	5	155	9.1	9	60	1.1	271	185	0.1	217	2649	1,533,084	
25°–54°	31.6	15	127	15.8	15	177	4.8	33	277	3.7	36	125	1,330,264	
<24°	26.6	29	51	22.2	28	54	3.1	29	97	21.3	1		585,536*	
<i>Reservoirs</i>														
>66°	0.2 [†]												35,289	
>54°–66°	1.0	24	176	1.8	2	140	0.2	4	93				161,352	
25°–54°	0.7 [‡]												116,922	
<24°	18.1	11	87										186,437	
<i>Rivers</i>														
>66°	0.1		1										38,895	
>54°–66°	0.2 [†]												80,009	
25°–54°	0.3	20	302										61,867	
<24°	0.9 [‡]												176,856	
Sum open water	93.1	116		55.3	71		9.9	397		25.1	254			
Plant flux	10.2													
Sum all	103.3													

- Total freshwater methane emission is 104 Tg yr^{-1} , i.e. 50% of global wetland emission ($177\text{--}284 \text{ Tg yr}^{-1}$, IPCC, 2013)
- greenhouse warming potentials from freshwater-originating CO_2 and CH_4 are roughly equal

CO₂ emissions by lakes and rivers

Raymond et al., 2013, Nature



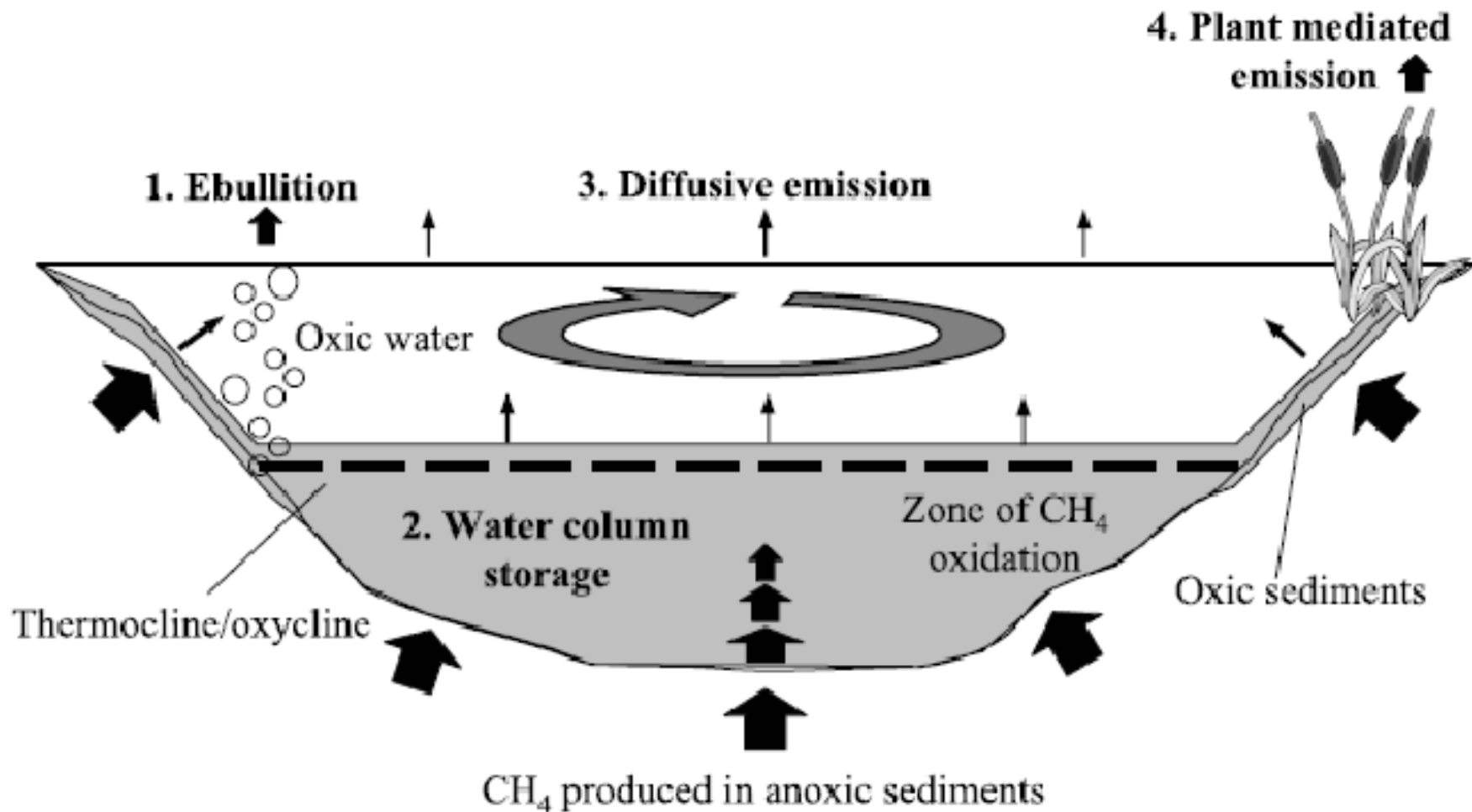
Lakes

- global emission of CO_2 by freshwaters is 2.1 Pg C yr^{-1}
- lake emission is 0.3 Pg C yr^{-1} , river emissions is 1.8 Pg C yr^{-1}
- significant contribution of Volga hydropower reservoirs

Rivers

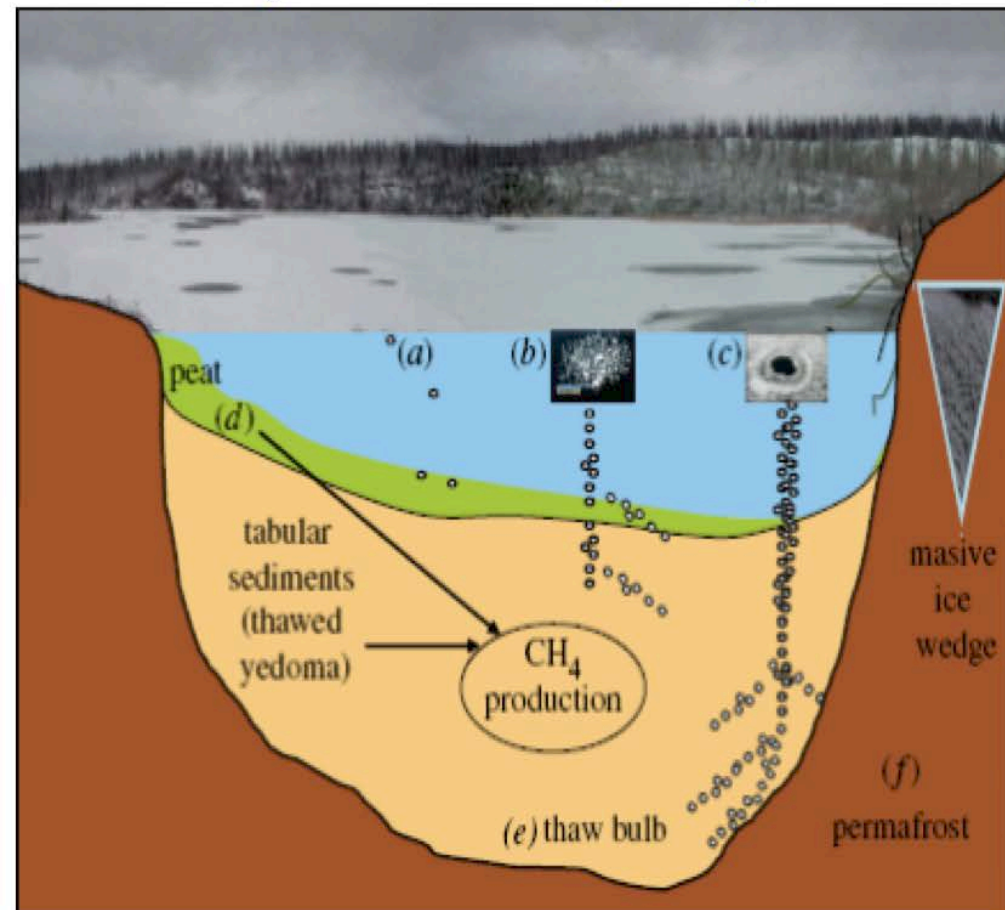
Methane production, consumption, transport and emission in lakes

(Bastviken et al., 2004)



Модель метана в донных отложениях

Генерация и перенос метана в
донных отложениях
термокарстового озера
(Walter et al., 2007)



Уравнение для концентрации метана в
донных отложениях (Walter and Heimann,
1996):

$$\frac{\partial C_{CH_4}}{\partial t} = \frac{\partial}{\partial z_s} \left(k_{CH_4} \frac{\partial C_{CH_4}}{\partial z_s} \right) + P_{soil,CH_4} - E_{soil,CH_4} - O_{soil,CH_4},$$

где P_{soil,CH_4} – производство метана в
донных отложениях :

$$P_{soil,CH_4,i} = P_{i,0} \rho_i^* H(T - T_{mp}) q_{10}^{T/10} * \\ * (1 + \alpha_{O_2,inhib} C_{O_2})^{-1}$$

Профиль плотности метанообразующей
органики:

– молодой органики

$$\rho_i^* = \exp(-\alpha_{new} z_s), \quad i = 1$$

– старой органики

$$\rho_i^* = 2 + \lambda_\rho - \sqrt{(1 + \lambda_\rho)^2 + \gamma_\rho (h_t^2 - z_s^2)}, \quad i = 2.$$

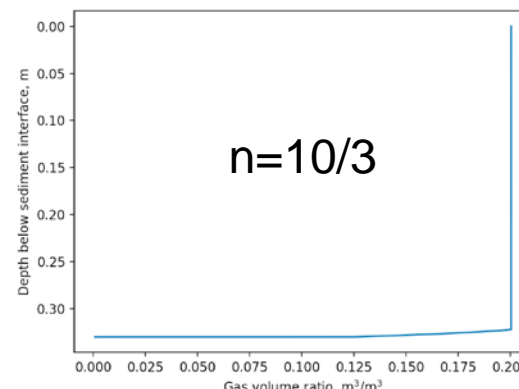
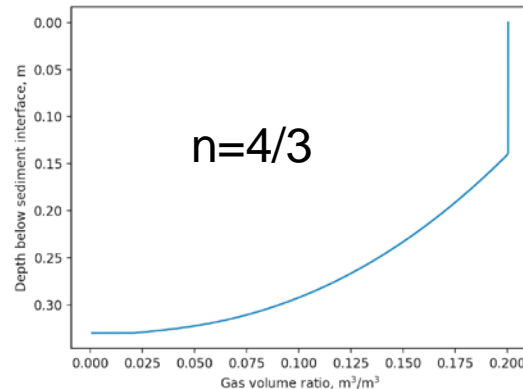
The role of bubbles trapped in sediments

Hypothesis: presence of bubbles in sediments significantly affects total CH₄ emission to atmosphere, **because gaseous diffusivity 4 orders large than aqueous one.**

The general aqueous and gaseous diffusion equation reduces to:

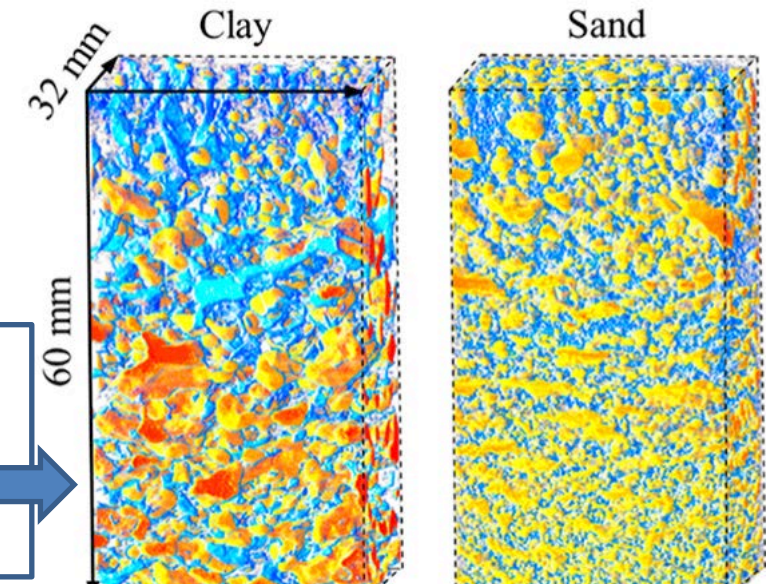
$$\frac{\partial \theta_g^{n+1}}{\partial z} + \tilde{S} + (z + z_1) \tilde{r}_{eb} (\theta_{g,cr} - \theta_g) = 0,$$

which is solved semi-analytically.

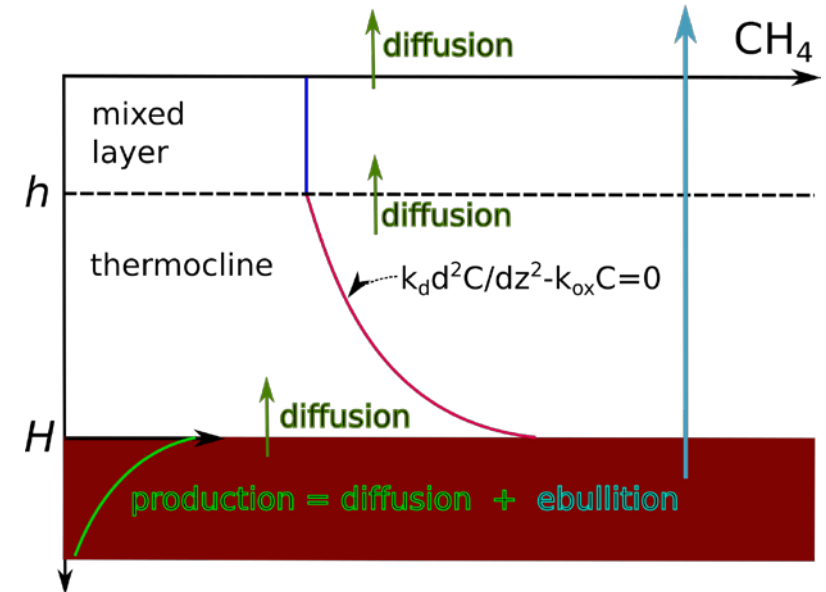


In a typical case of bubbles trapped in sediments, bubble volume becomes a measure of vertical diffusive flux.

X-ray tomography of bubbles in sediments



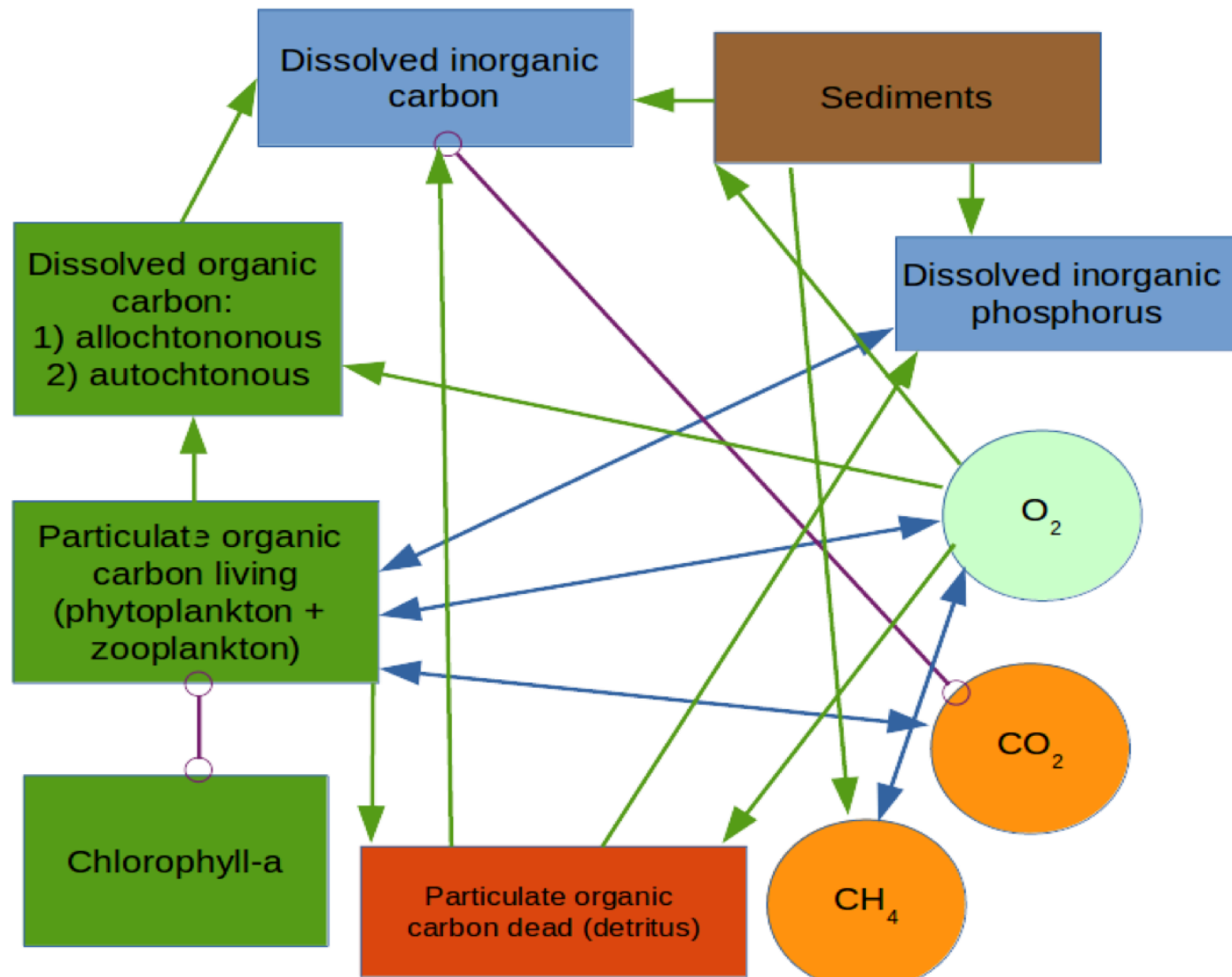
(Liu et al., 2018)



Biogeochemical interactions in the model

(Stepanenko et al., FAC, 2020)

- Photosynthesis, respiration and BOD are empirical functions of temperature, Chl-a and phosphorus
- Oxygen uptake by sediments (SOD) is controlled by O_2 concentration and temperature (Walker and Snodgrass, 1986)
- Methane production $\propto P_0 q_{10}^{T-T_0}$, P_0 is calibrated (Stepanenko et al., 2011)
- Methane oxidation follows Michaelis-Menthen equation



Bubble model

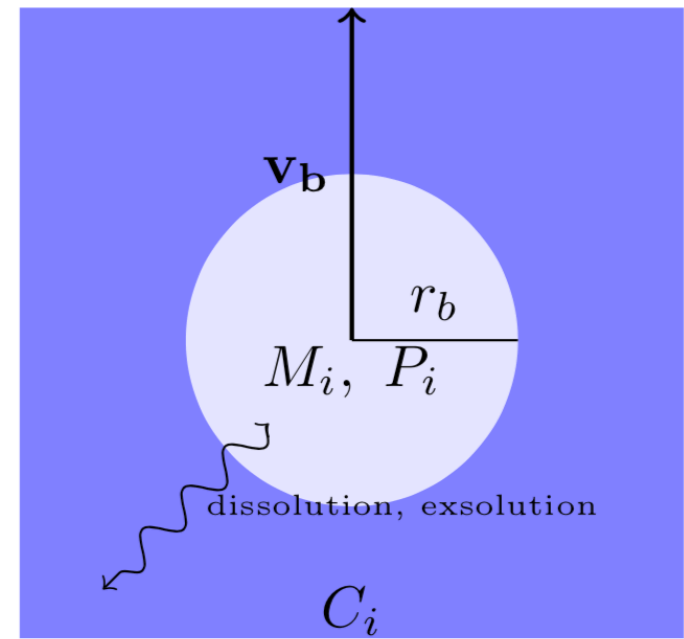
For shallow lakes (several meters), bubbles reach water surface not affected, for deeper lakes bubble dissolution has to be taken into account.

- Five gases are considered in a bubble:
 CH_4, CO_2, O_2, N_2, Ar
- Bubbles are composed of CH_4 and N_2 when they are emitted from sediments
- The velocity of bubble, v_b , is determined by balance between buoyancy and friction
- The molar quantity of i -th gas in a bubble, M_i , changes according to gas exchange equation (McGinnis et al.,

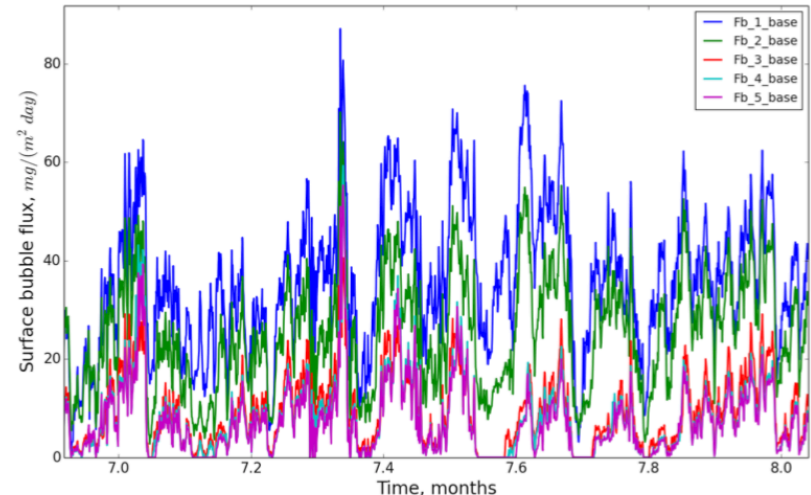
$$\frac{dM_i}{dt} = v_b \frac{\partial M_i}{\partial z} = -4\pi r_b^2 K_i (H_i(T) P_i - C_i).$$

- Gas exchange with solution is included in conservation equation for i -th gas :

$$\frac{\partial C_i}{\partial t} = \frac{1}{A} \frac{\partial}{\partial z} Ak \frac{\partial C_i}{\partial z} + \frac{1}{A} \frac{\partial AB_{C_i}}{\partial z} + F(z, t, C_i, A) + (H_{C_i} - B_{C_i, b}) \frac{1}{A} \frac{dA}{dz}.$$

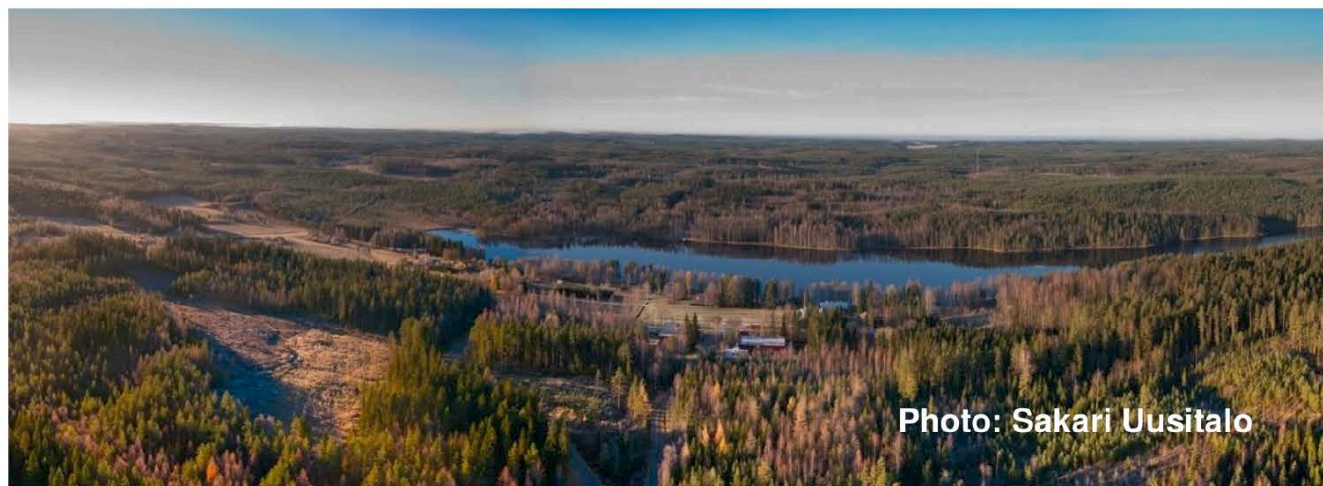
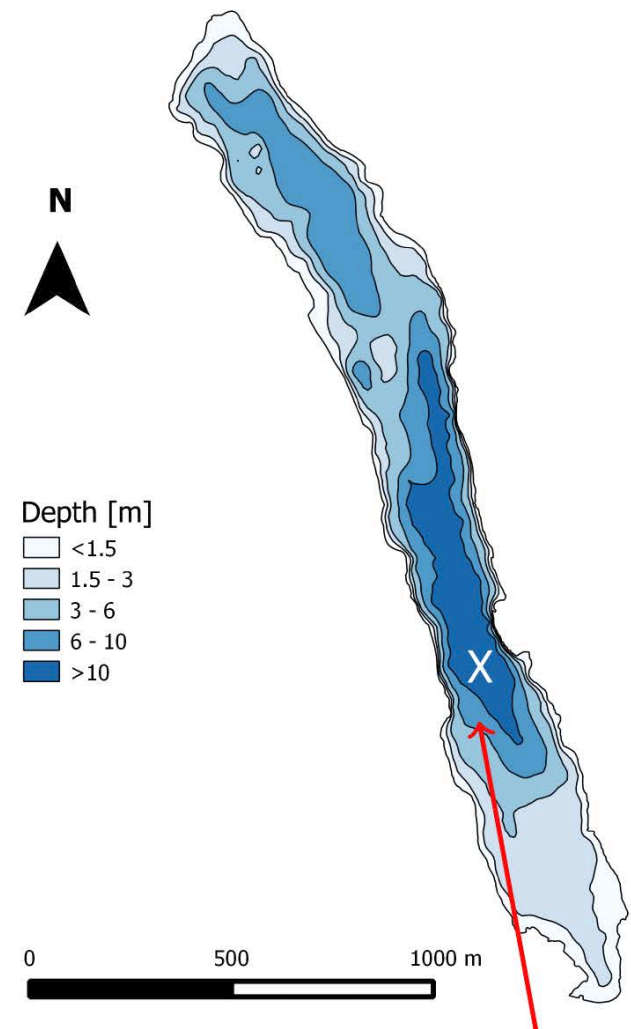
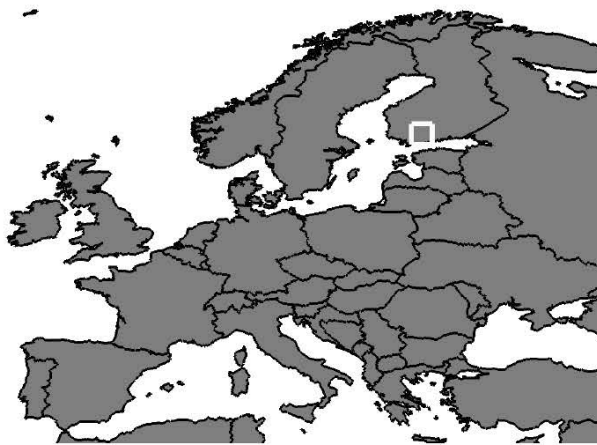


Methane ebullition
from different soil columns



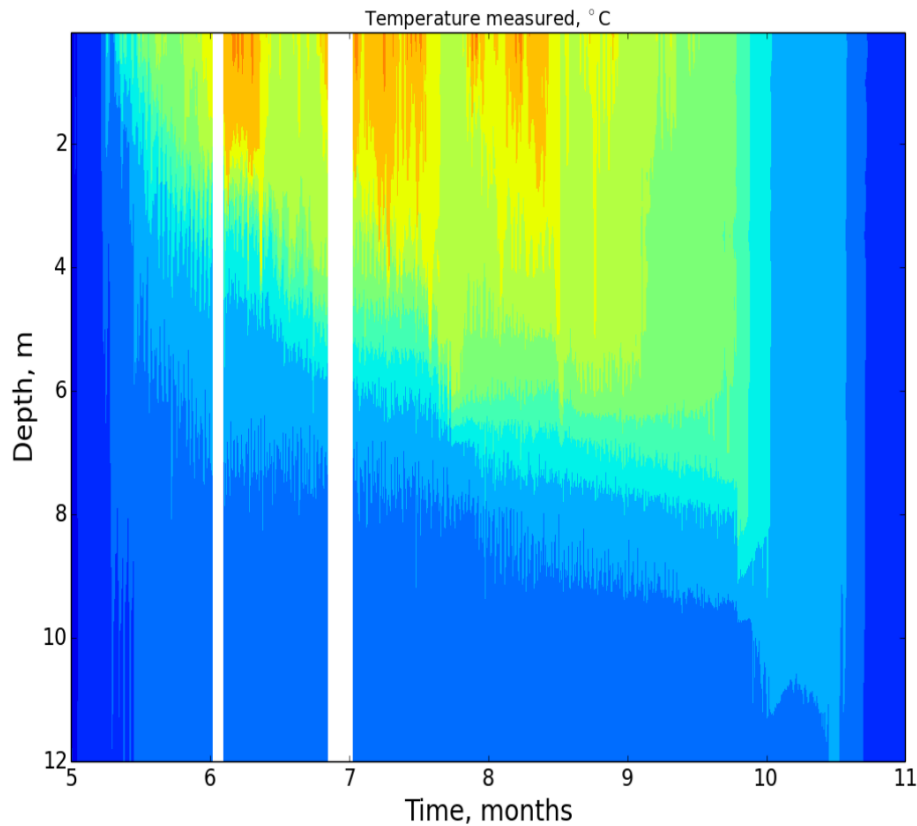
Kuivajärvi Lake (Finland)

- Mesotrophic, dimictic lake
- Area 0.62 km^2 (length 2.6 km, modal fetch 410 m)
- Altitude 142 m a.s.l.
- Maximal depth 13.2 m, average depth 6.4 m, deptl the point of measurements 12.5 m
- Catchment area 9.4 km^2

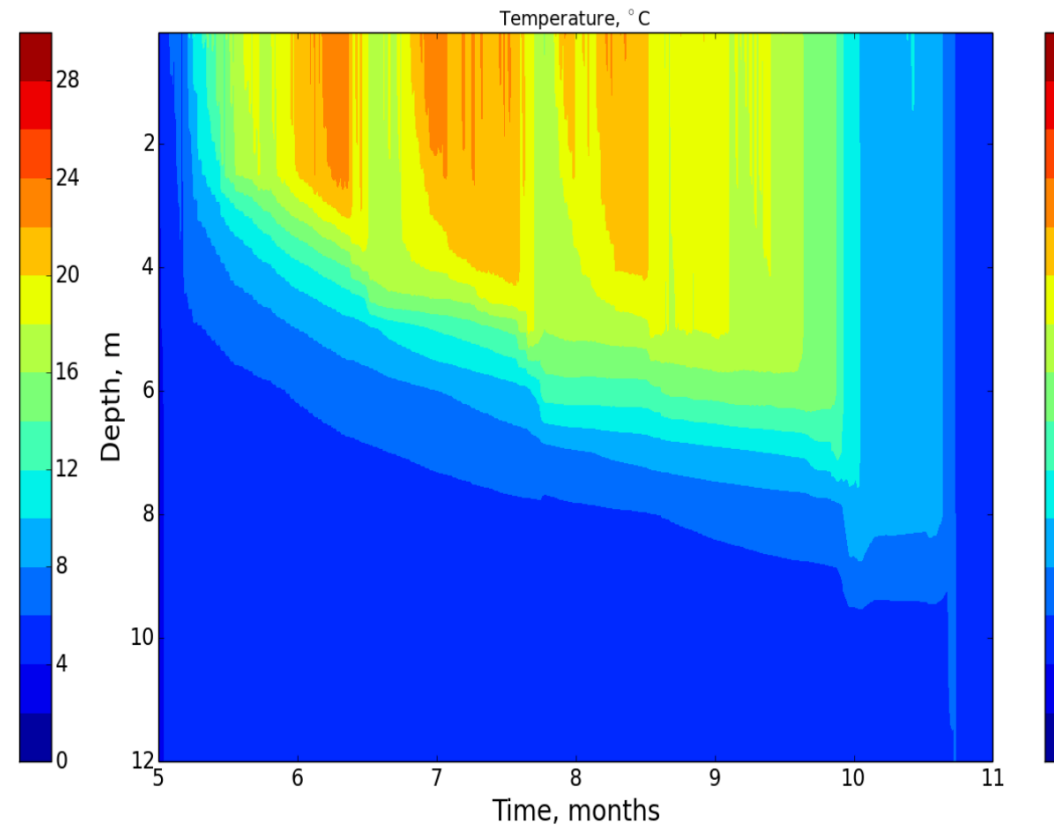


Water temperature

Measurements



Model

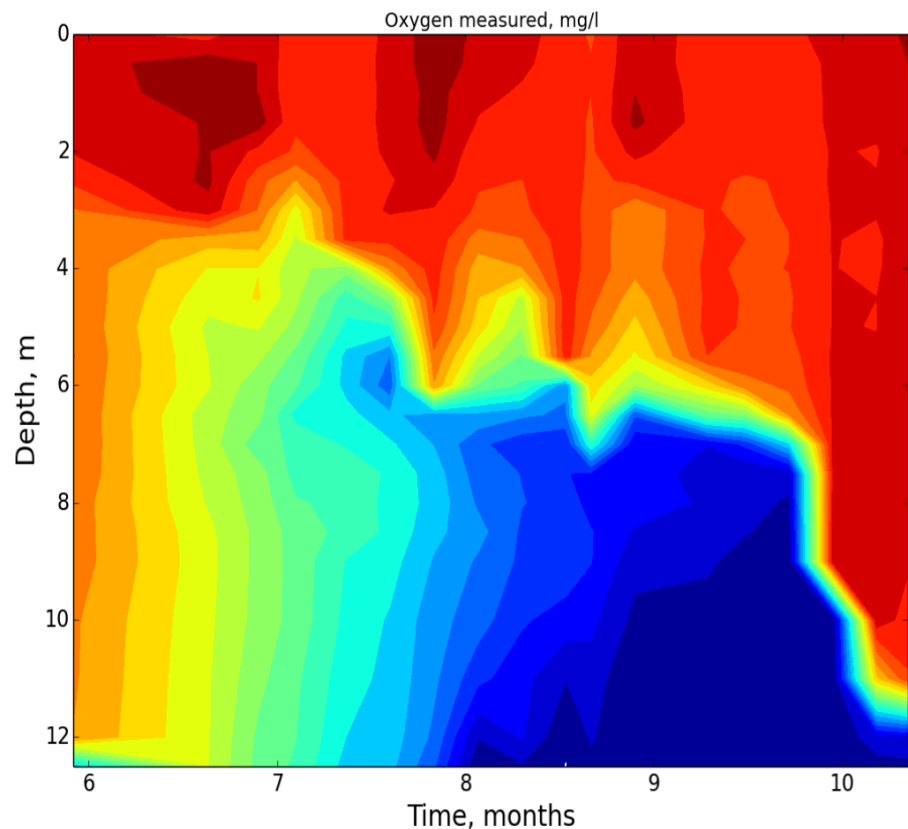


- Mixed layer depth and surface temperature ($\text{RMSE}=1.54 \text{ }^{\circ}\text{C}$) are well reproduced
- Stratification strength in the thermocline is overestimated
- Model results lack frequent temperature oscillations in the thermocline

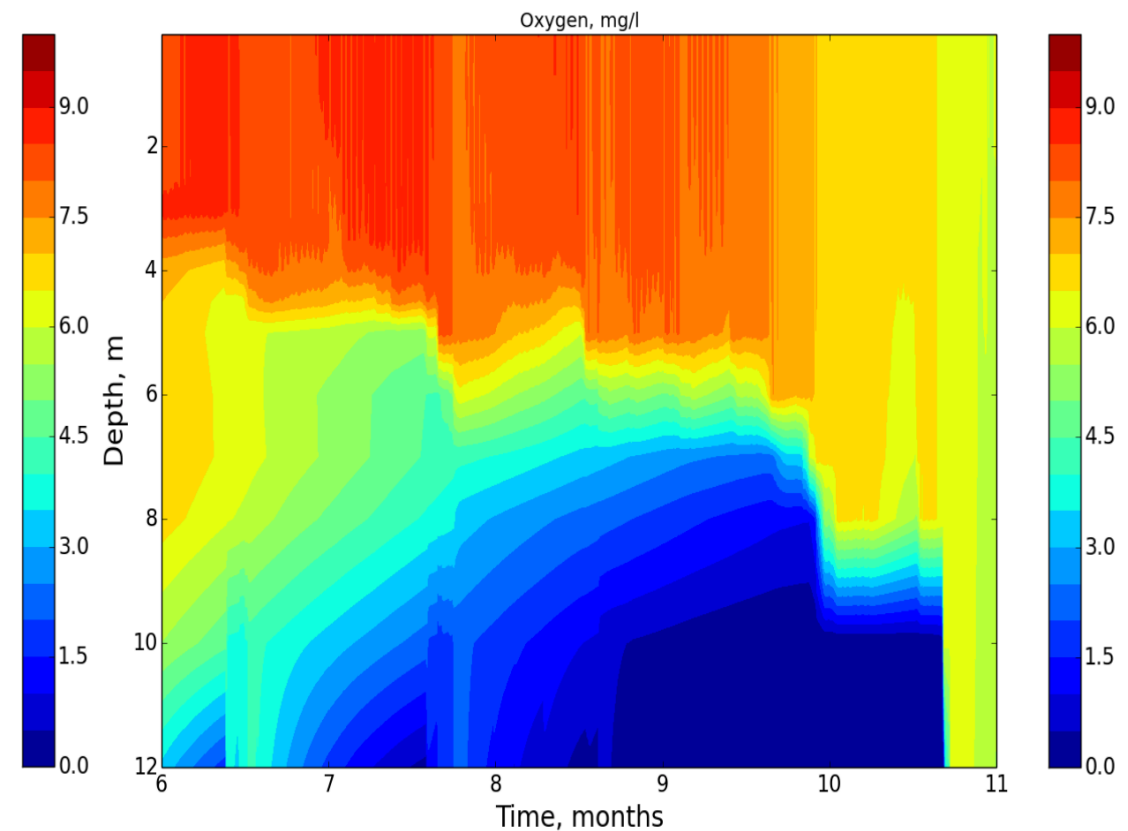
Oxygen

Stepanenko et al., Geosci. Mod. Dev., 2016

Measurements



Model

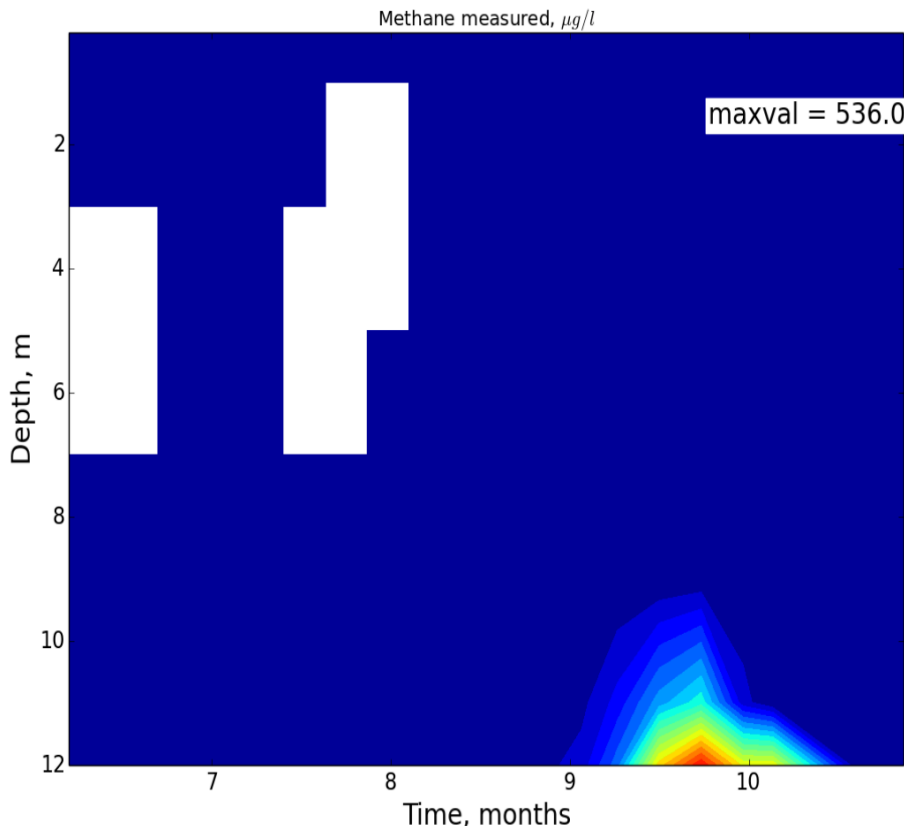


- Seasonal pattern is well captured: oxygen is **produced** in the mixed layer and **consumed** below
- Oxygen concentration in the mixed layer is underestimated by 1-1.5 mg/l , and more significantly during autumn overturn

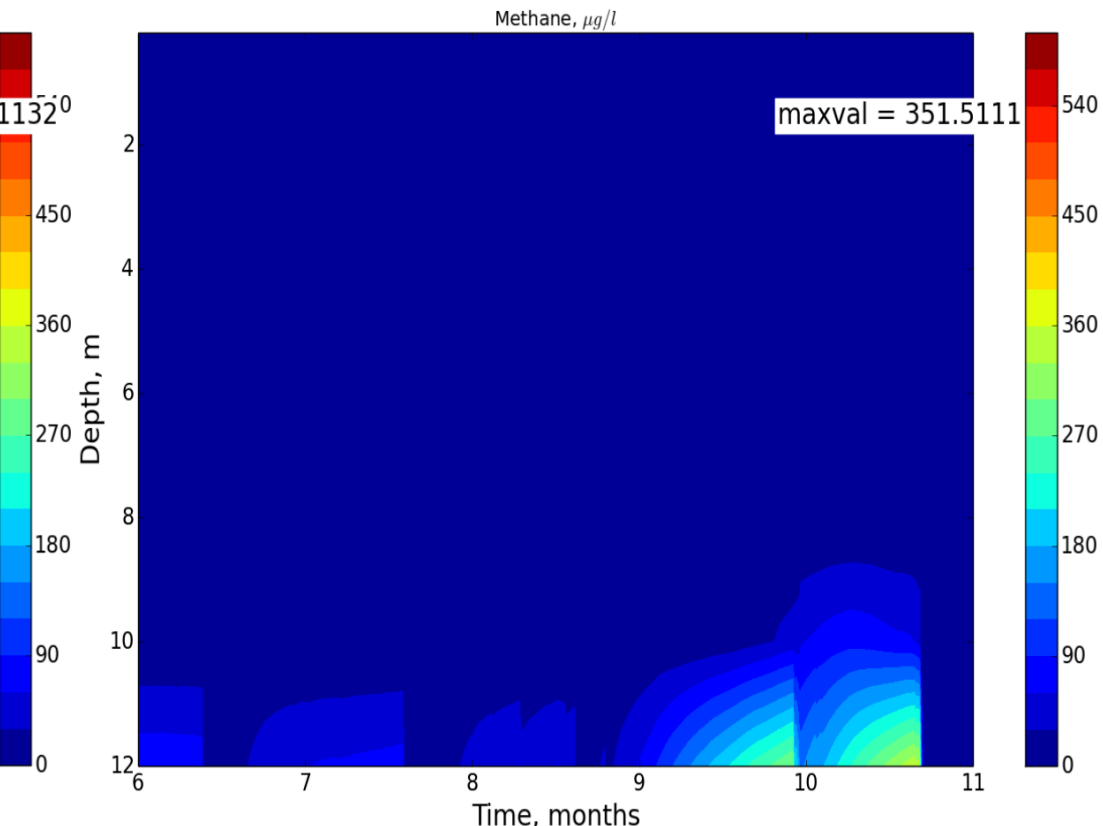
Methane

Stepanenko et al., Geosci. Mod. Dev., 2016

Measurements



Model

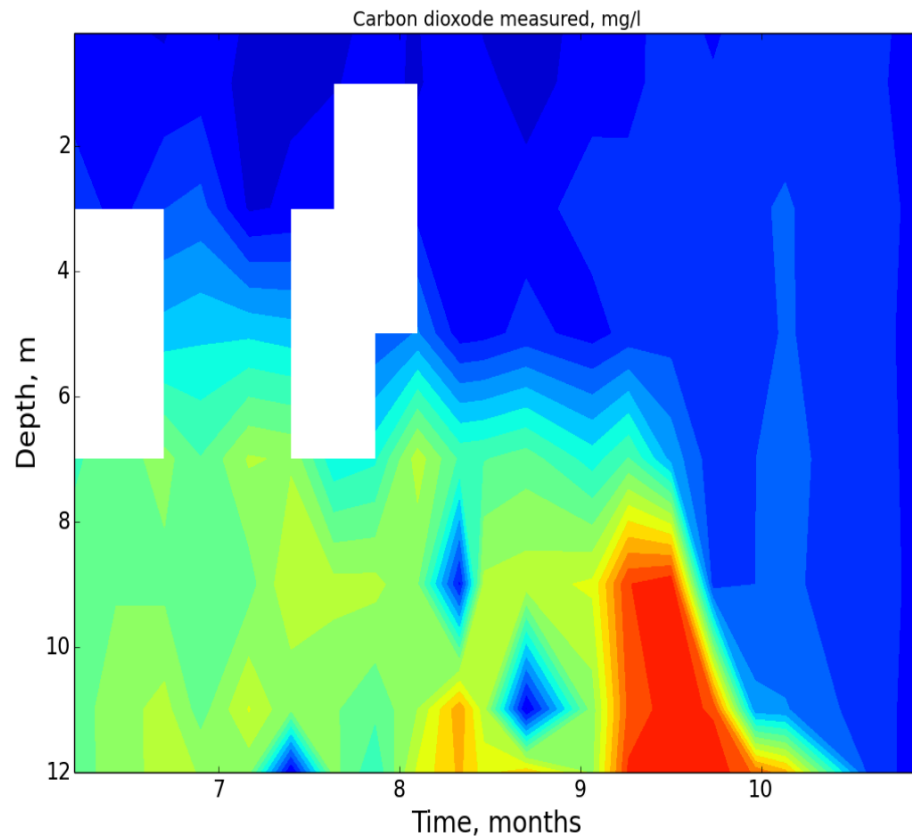


- Methane starts to accumulate near bottom in the late summer when oxygen concentration drops to low values
- Surface methane concentration is very small leading to negligible diffusive flux to the atmosphere, consistent with measurements

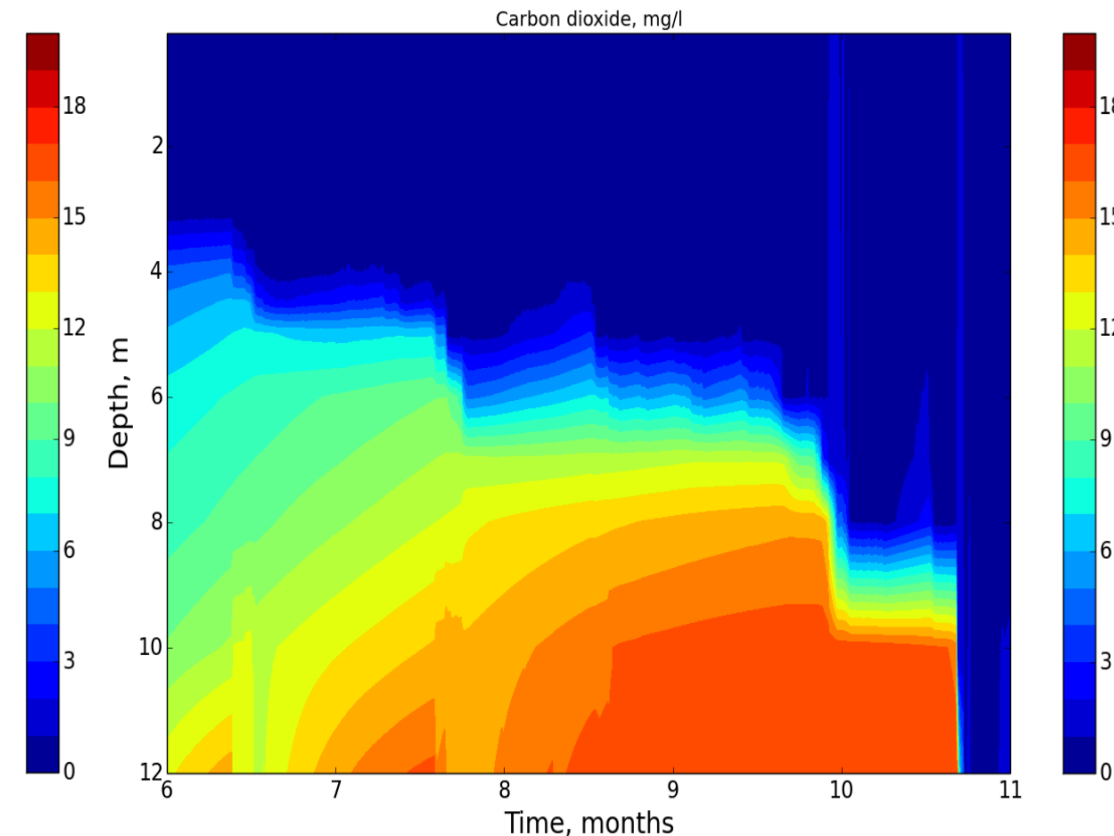
Carbon dioxide concentration

Stepanenko et al., Geosci. Mod. Dev., 2016

Measurements



Model



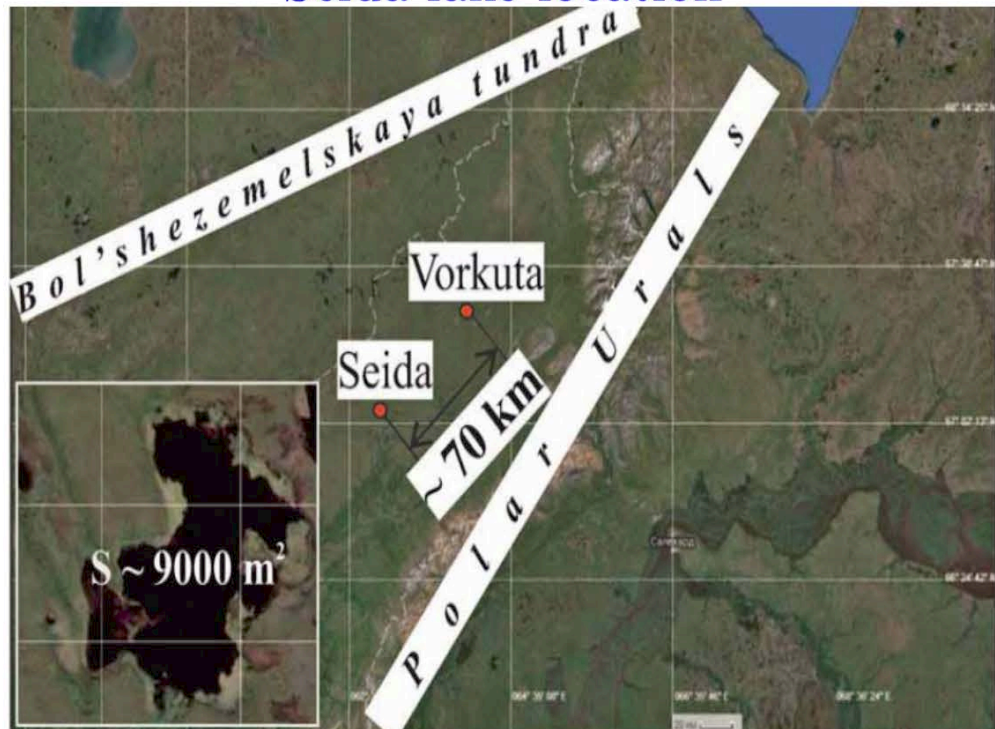
- Seasonal pattern is simulated realistically: carbon dioxide is **consumed** by photosynthesis in the mixed layer and **produced** in the thermocline and hypolimnion by aerobic organics decomposition
- Sudden CO_2 increase prior to autumn overturn is absent in the model



Model validation for Seida Lake

Guseva et al., Geogr. Env. Sust., 2016

Seida lake location



Bubble flux (starting from 01.07.2007)

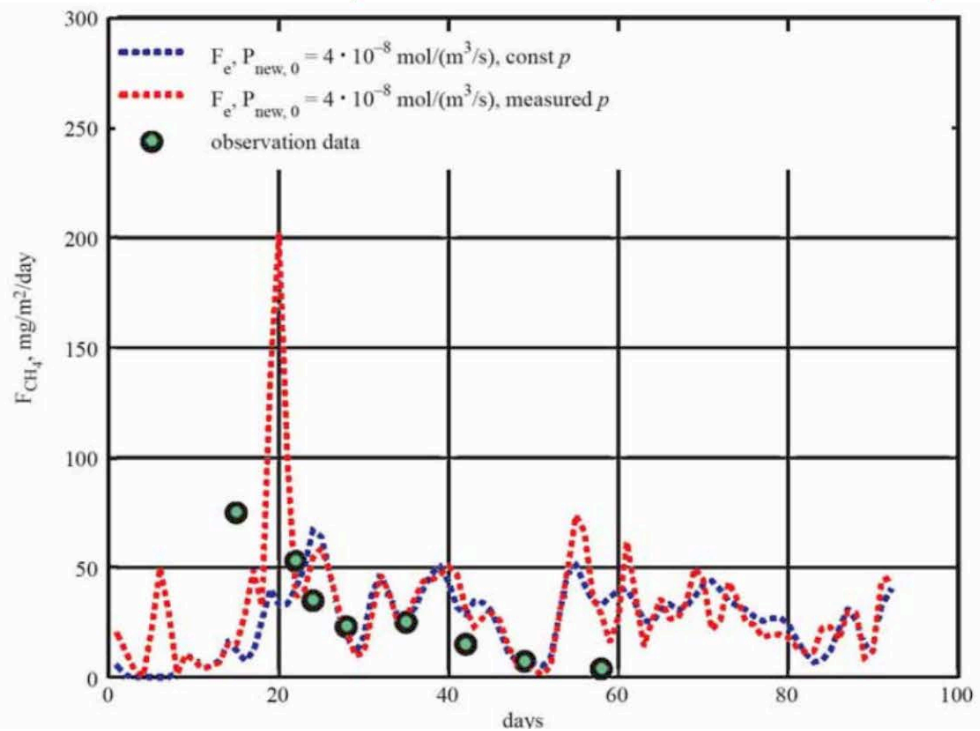


Table 3. Methane production rate constant $P_{\text{new}, 0}$ in other studies

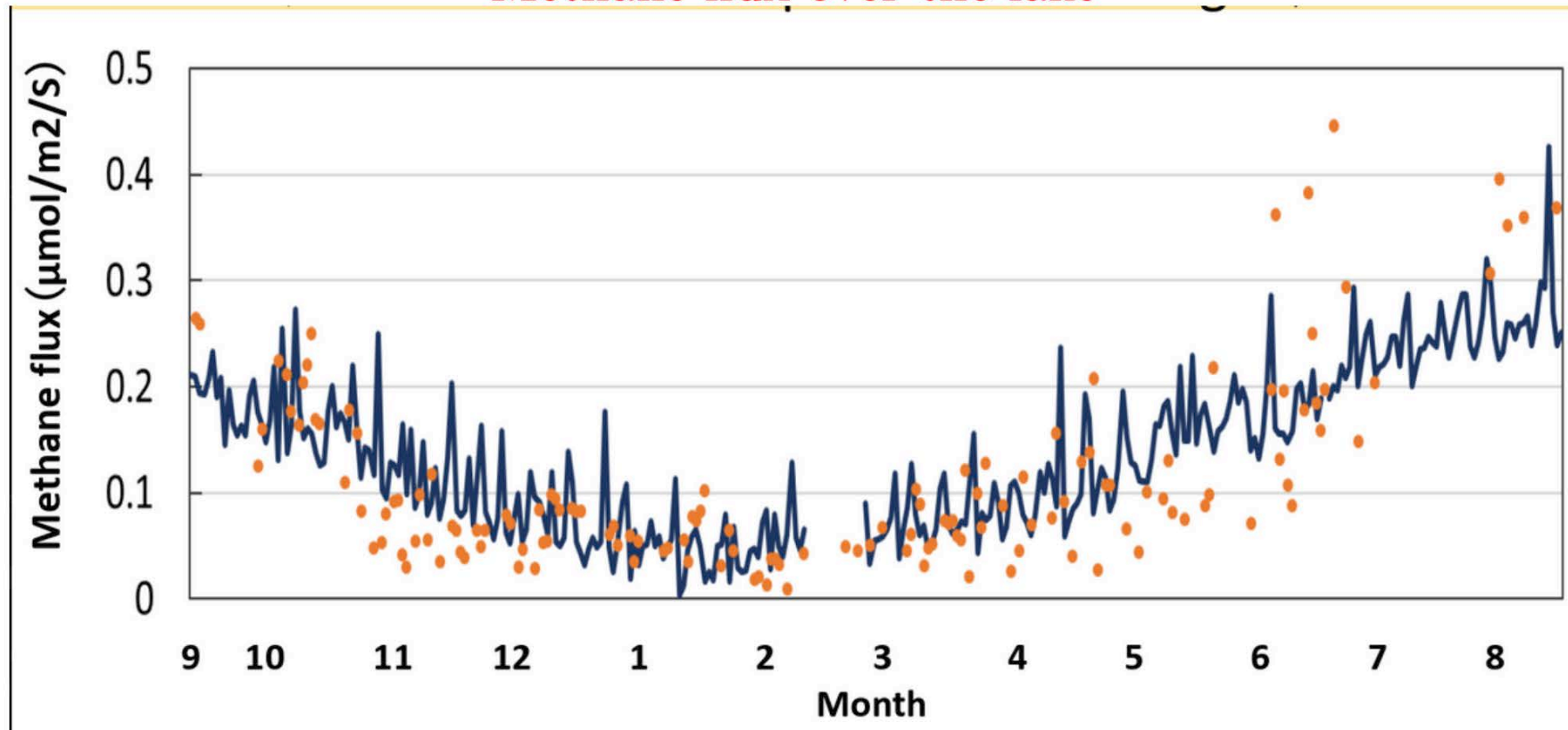
$P_{\text{new}, 0} (\text{mol} \cdot \text{m}^{-3} \cdot \text{s}^{-1})$	Source
$3.0 \cdot 10^{-8}$	Lake Kuivajarvi, Finland [Stepanenko et al., 2016]
$2.55 \cdot 10^{-8}$	Shuchi Lake, North Eastern Siberia, Russia [Stepanenko et al., 2011]
$8.3 \cdot 10^{-8} - 1.6 \cdot 10^{-7}$	High latitude wetlands [Walter & Heimann, 2000]
$4.0 \cdot 10^{-8}$	Lake at the Seida site, current study

Methane emission from Suwa Lake (Japan)

Simulations with LAKE by H.Iwata group in Nagano University

Lake sizes 3 km×4 km. Maximal depth 7 m.

Methane flux over the lake



Methane production constant P_0 and maximal oxidation rate V_{max}
are measured in lab.



Global estimates of GHGs from reservoirs

Hydropower is no more thought as greenhouse-gas-free energy source



Global synthesis of GHG emissions from artificial reservoirs (Deemer et al., 2016):

Table 1. The global surface area and GHG flux estimates from reservoirs compared with those of other freshwater ecosystems and other anthropogenic activities.

System Type	Surface Area ($\times 10^6 \text{ km}^2$)	Annual teragrams (Tg)			Areal Rates (milligrams per square meter per day)			Annual CO ₂ Equivalents (Tg CO ₂ Eq per year)			
		CH ₄ -C	CO ₂ -C	N ₂ O-N	CH ₄ -C	CO ₂ -C	N ₂ O-N	CH ₄	CO ₂	N ₂ O	Total
All Reservoirs (This Study)	0.31 ^a	13.3	36.8	0.03	120	330	0.30	606.5	134.9	31.7	773.1
All Reservoirs (Other Work)	0.51–1.5 ^{b,c}	15–52.5 ^{b,d}	272.7 ^b	–	82–96	498	–	680–2380	1000	–	–
Hydroelectric Reservoirs	0.34 ^e	3–14 ^{e,f}	48–82 ^{e,f}	–	24–112	386–660	–	136–635	176–301	–	–
Lakes	3.7–4.5 ^{g,h}	53.7 ^d	292 ^g	–	40	216	–	2434	1071	–	–
Ponds	0.15–0.86 ⁱ	12 ⁱ	571 ⁱ	–	27 ⁱ	422 ⁱ	–	544	2094	–	–
Rivers	0.36–0.65 ^{d,e}	1.1–20.1 ^{d,j}	1800 ^g	–	6–98 ^j	7954	–	50–911	6600	–	–
Wetlands	8.6–26.9 ^k	106–198 ^k	–	0.97 ^l	15–63 ^k	–	0.1–0.31	4805–8976	–	908	–
Other Anthropogenic Emissions (2000s)	N.A.	248 ^m	9200 ^m	6.9 ^m	–	–	–	11243	33733	6462	51438

Note: The values presented are mean estimates; the ranges of mean values are reported when there are multiple relevant models. In cases in which the areal rates are not referenced, they were derived from dividing annual teragrams (Tg) of C or N by the global surface-area estimate. The annual CO₂ equivalents were calculated by multiplying the mass-based flux (in units of Tg CH₄, CO₂ or N₂O per year) by the 100-year global warming potential of each gas (1 for CO₂, 34 for CH₄ and 298 for N₂O). ^a (Lehner et al. 2011). ^b (St. Louis et al. 2000). ^c (Downing and Duarte 2009). ^d (Bastviken et al. 2011). ^e (Barros et al. 2011). ^f (Li and Zhang 2014). ^g (Raymond et al. 2013). ^h (Verpoorter et al. 2014). ⁱ (Holgerson and Raymond 2016). ^j (Stanley et al. 2016). ^k (Melton et al. 2013). ^l (Tian et al. 2015). ^m (Ciais et al. 2013).

GHG Measurement Guidelines for Freshwater Reservoirs

Derived from:
The UNESCO/IHA Greenhouse Gas Emissions from Freshwater Reservoirs Research Project



IPCC view on the problem

The screenshot shows a web browser displaying the IPCC website at <https://www.ipcc.ch/report/2019-refinement-to-the-2006/>. The page features a large banner image of a landscape with clouds. Overlaid on the banner is the title "2019 Refinement to the 2006 IPCC Guidelines for National Greenhouse Gas Inventories". In the top right corner of the banner, there is a "REPORT" button. The top navigation bar includes links for REPORTS, WORKING GROUPS, ACTIVITIES, NEWS, and CALENDAR, along with social media sharing icons.

Slide 1

2019 Refinement to the 2006 IPCC Guidelines for National Greenhouse Gas Inventories

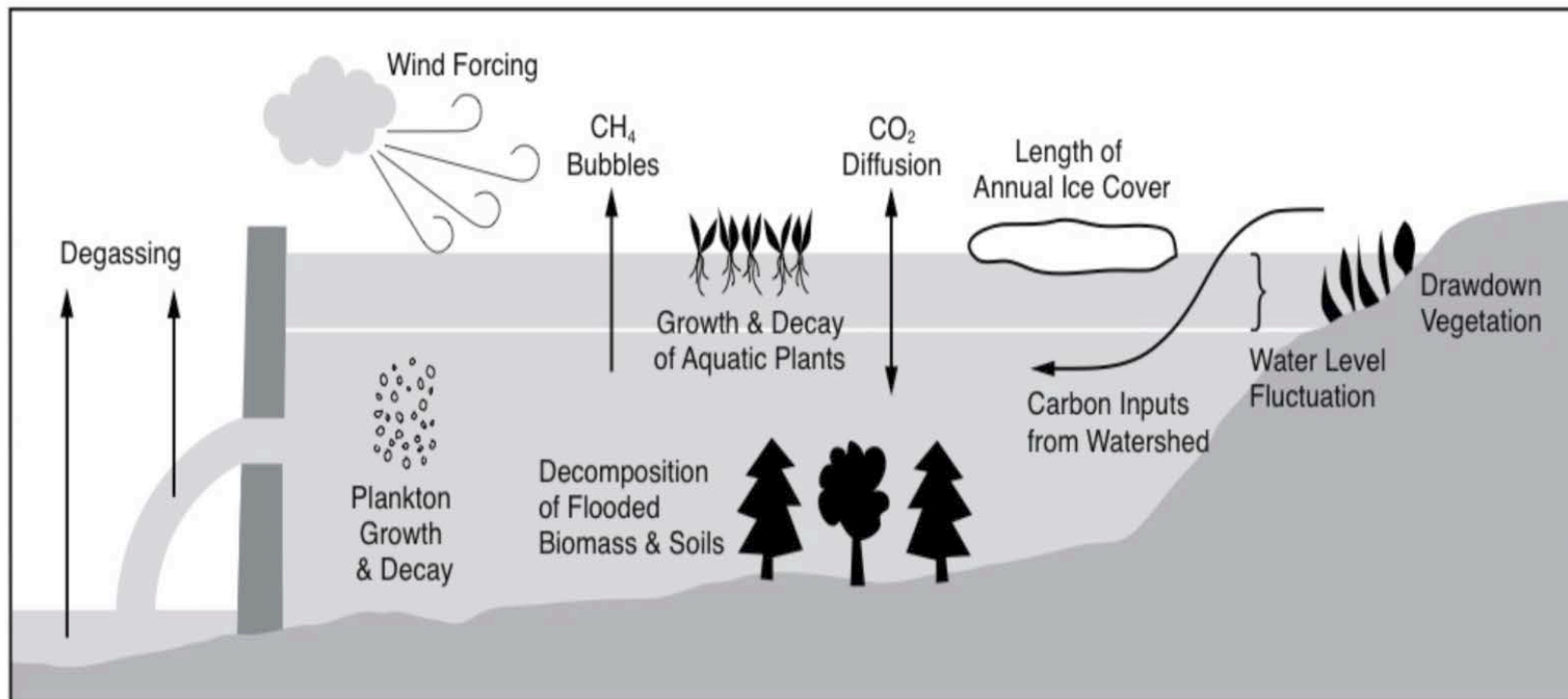
2019 Refinement to the 2006 IPCC Guidelines for
National Greenhouse Gas Inventories

TABLE 7.7
(NEW) TYPES OF FLOODED LAND, THEIR HUMAN USES AND GREENHOUSE GAS EMISSIONS CONSIDERED IN THIS CHAPTER

Flooded Land types	Human Uses	Greenhouse gas emissions for which guidance is provided in this Chapter
Reservoirs (including open water, drawdown zones, and degassing/downstream areas)	Hydroelectric Energy Production, Flood Control, Water Supply, Agriculture, Recreation, Navigation, Aquaculture	CO ₂ , CH ₄
Canals	Water Supply, Navigation	CH ₄
Ditches	Agriculture (e.g. irrigation, drainage, and livestock watering)	CH ₄
Ponds (Freshwater or Saline)	Agriculture, aquaculture, recreation	CH ₄



Emission of greenhouse gases from reservoirs



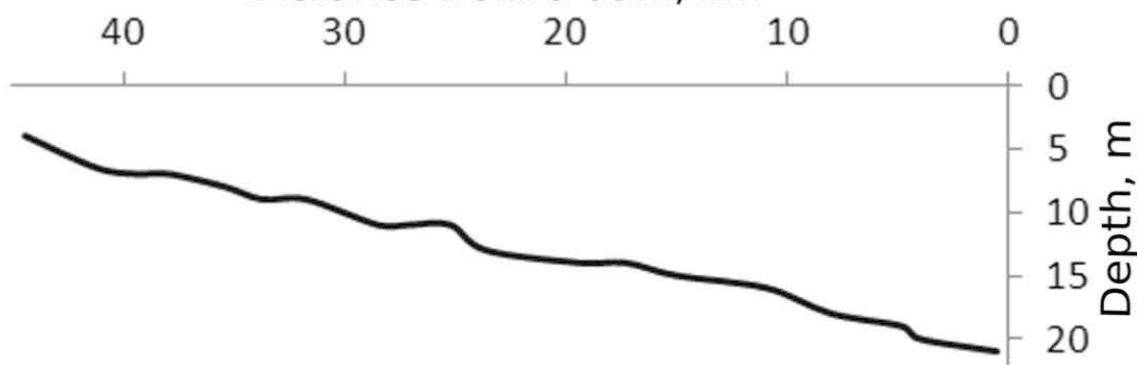
- Artificially flooded ecosystems are imposed to both aerobic (producing CO₂) and anaerobic (producing CH₄) degradation
- Compared to natural lakes there is an additional pathway of gases that is through turbines

Mozhayskoe reservoir

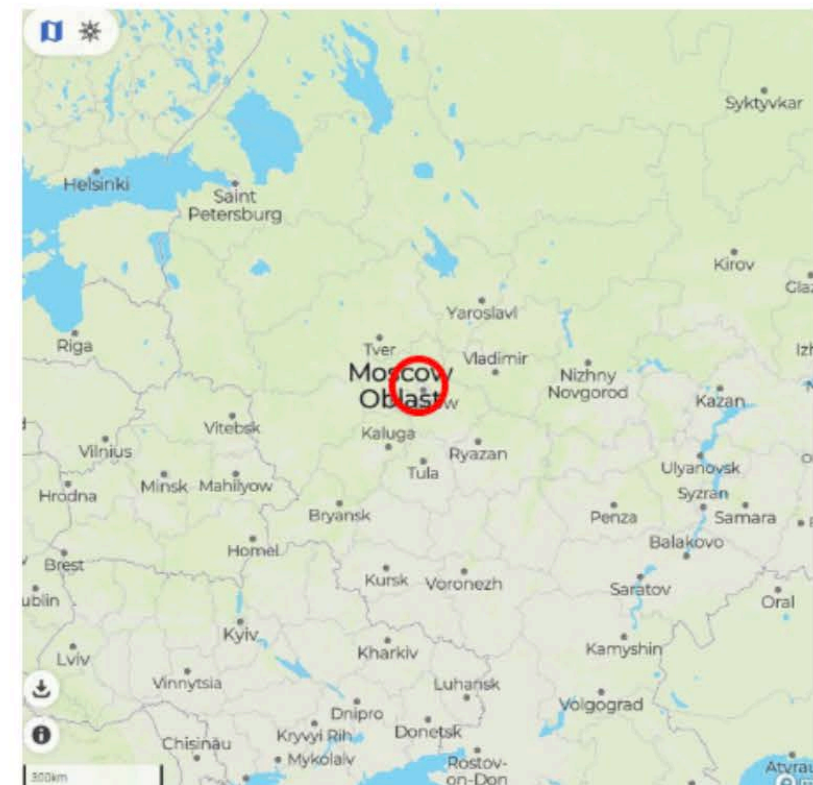


Depth of an impounded river bed

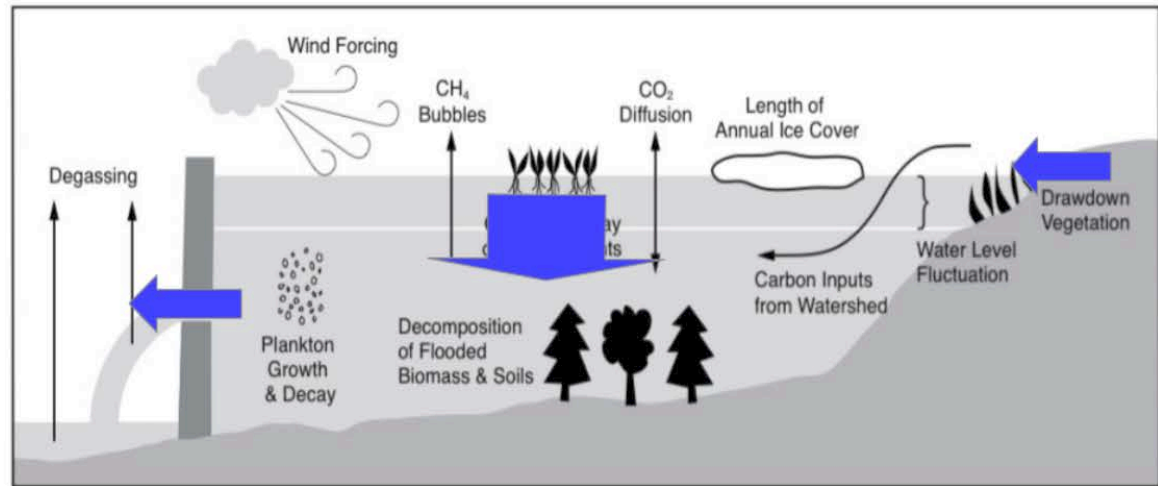
Distance from a dam, km



- length 47 km, width up to 3.5 km, max. depth 23 m
- water residence time 0.8 yr
- hydropower station and drinking water supply



Inflow, outflow and advection



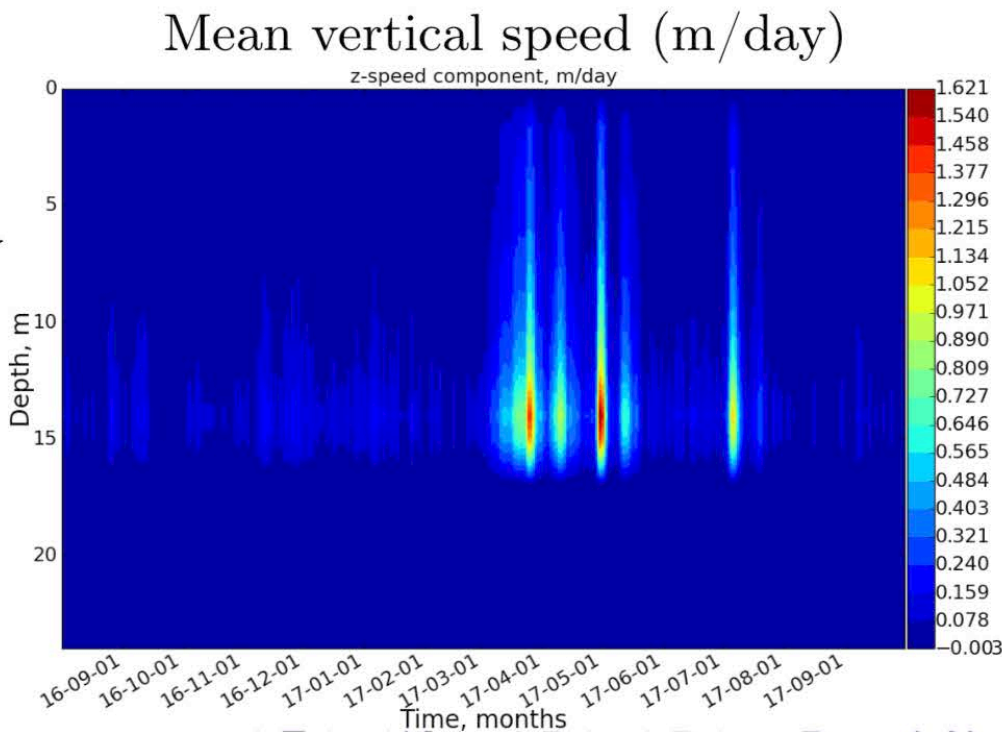
- Inflow and outflow are accounted for as source and sink of physical and biogeochemical variables
- The difference in the depth of water input and output leads to the large-scale water

Continuity equation allows to compute vertical speed w :

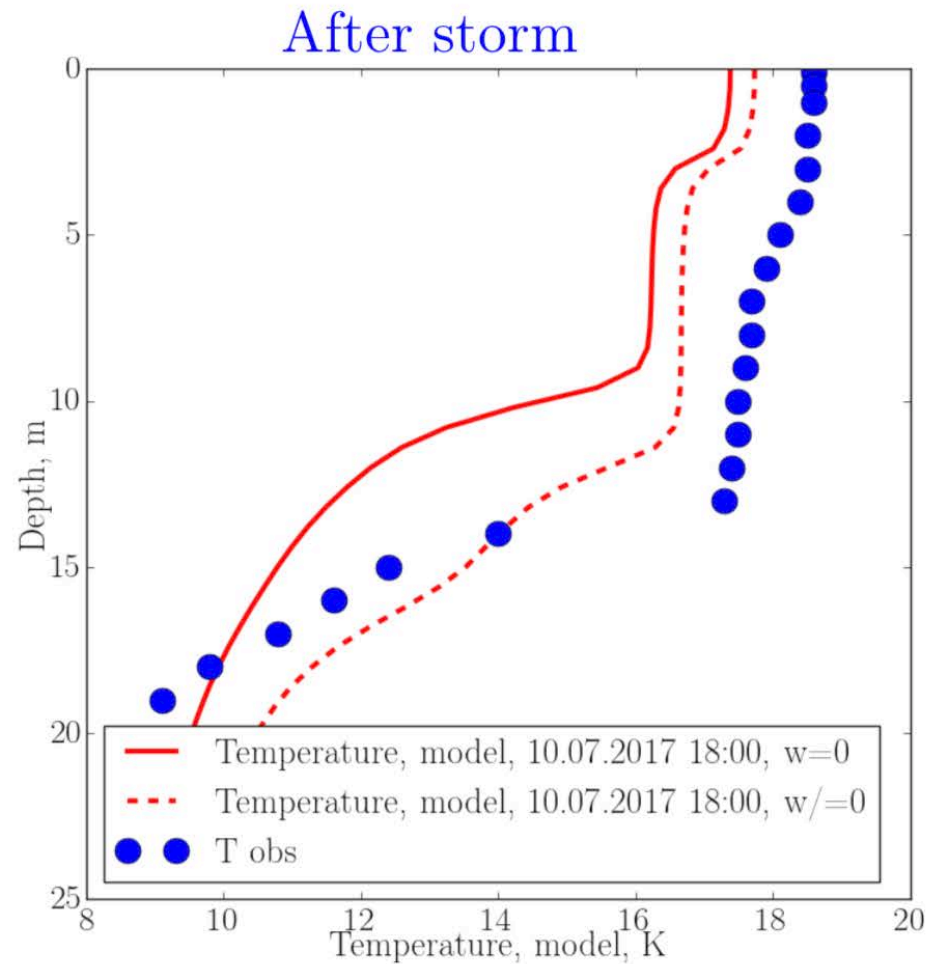
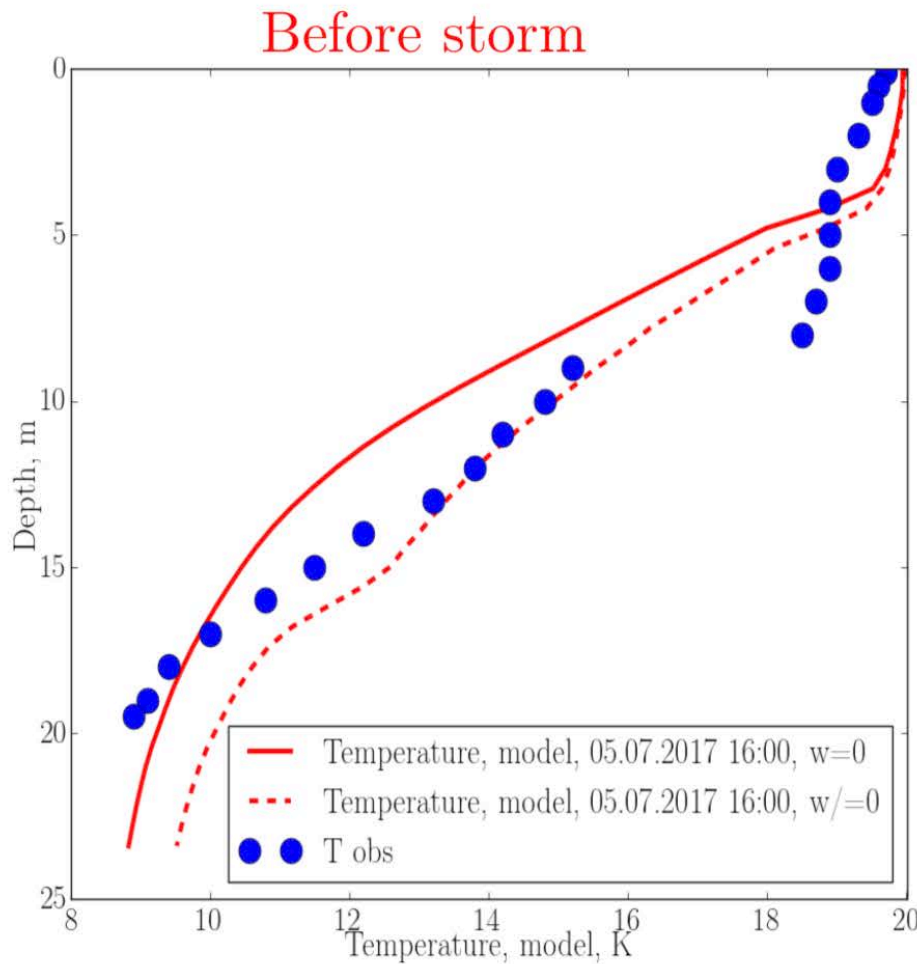
$$\frac{\partial \bar{w} A}{\partial z} = - \int_{\Gamma_A(z)} (\mathbf{u}_h \cdot \mathbf{n}) dl = \text{Inflow} - \text{Outflow}$$

Vertical advection is added to a balance equation of each scalar:

$$c \frac{\partial f}{\partial t} = - \frac{c}{A} \frac{\partial \bar{w} A \bar{f}}{\partial z} + \dots$$



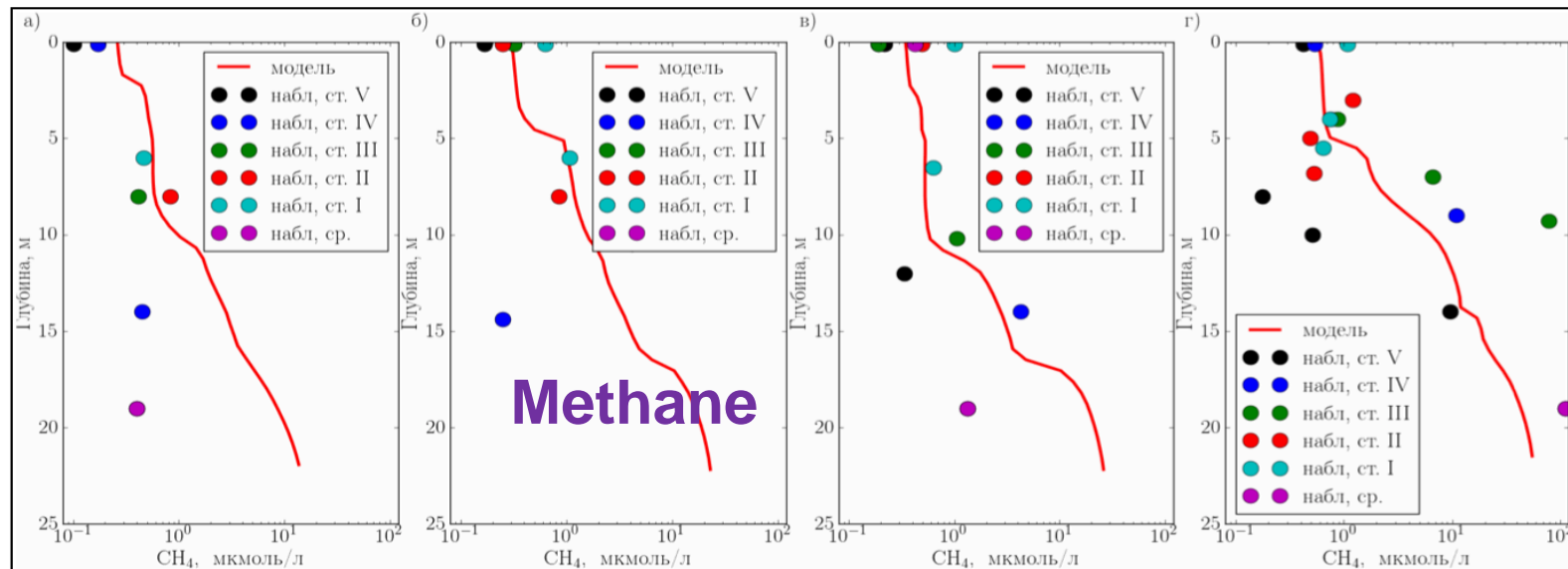
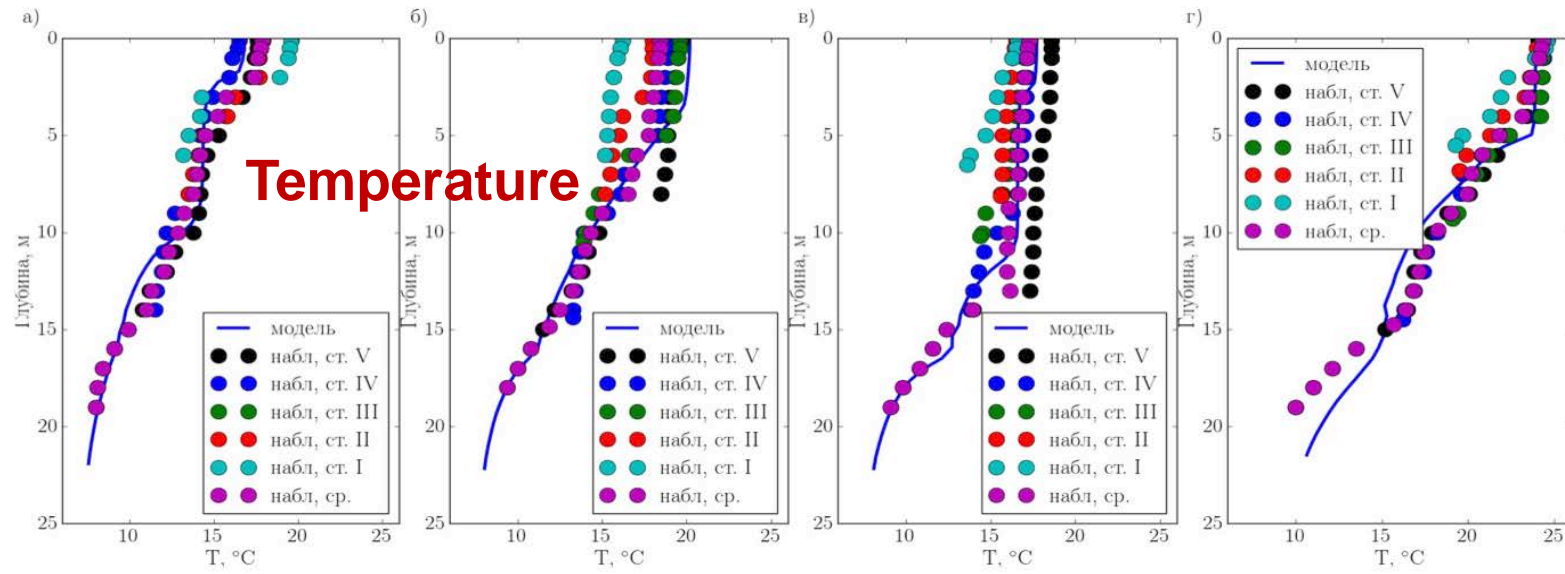
Temperature: effect of vertical advection



- High wind speeds (6-8 m/s) and rainfall persisted over 4 days, causing river discharge to reach $70 \text{ m}^3/\text{s}$ (contrasting to $5-10 \text{ m}^3/\text{s}$ before and after event)
- The mixed-layer deepening is much better reproduced when including vertical advection

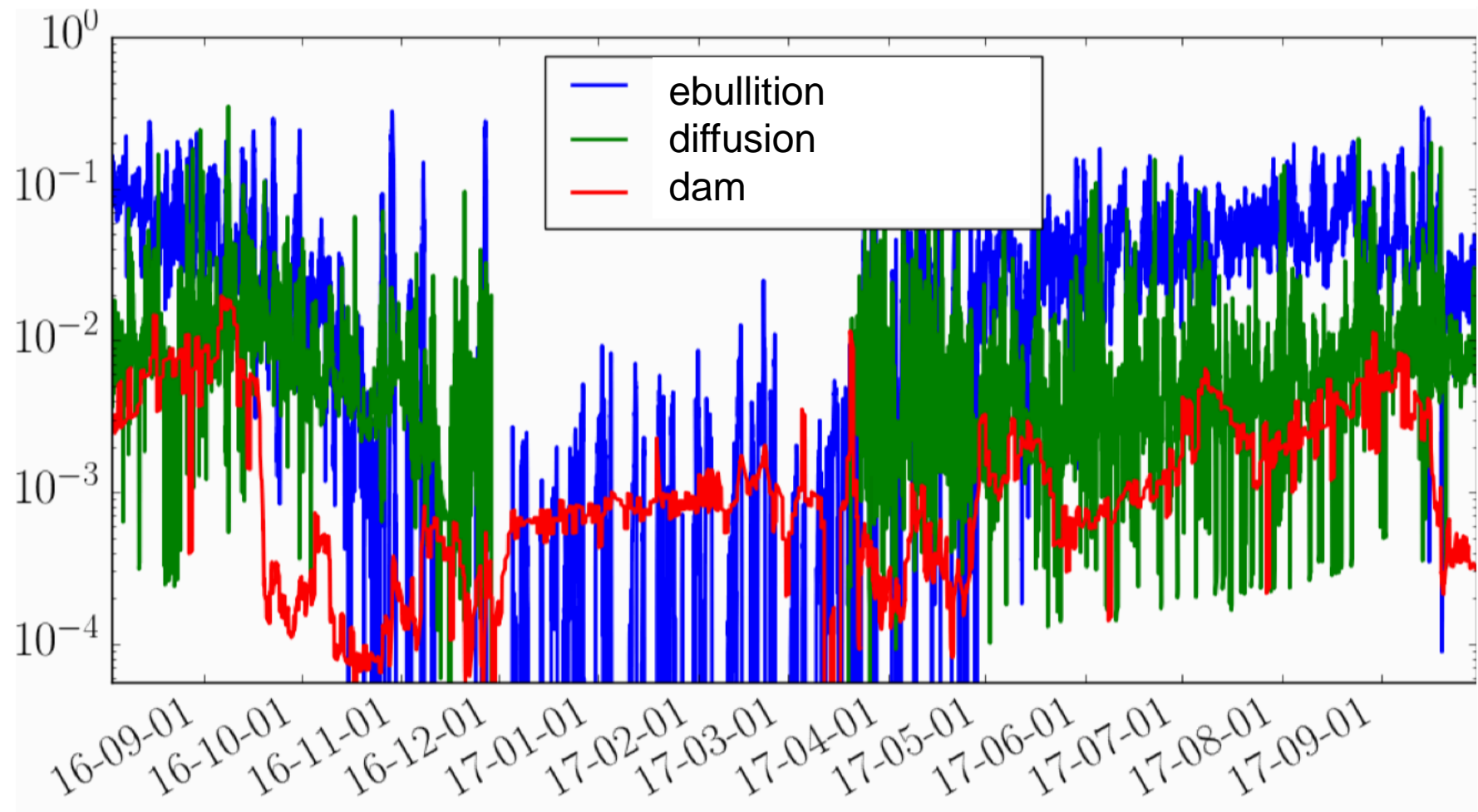


Vertical distribution of temperature and methane in the Mozhaisk reservoir: summer 2017 (Stepanenko et al., 2020)



Results with Mozhayskoe reservoir

mcmol/(m²*s)



Total CH₄ flux from 1 August 2016 till 1 August 2017 is 570 Mt, where:

- ebullition 455 Mt/yr (80%),
- diffusion 87 Mt/yr (15%),
- dam flux 28 Mt/yr (5%).

ISIMIP3: lake methane sector

Requirements for the validation sites

VARIABLE NAME	UNIT	RESOLUTION	COVERAGE	PRIORITY (1 is highest priority)	MANDATORY/ OPTIONAL
LAKE TEMPERATURE (profiles)	K	daily or monthly	> 2 years	1	M
Total CH ₄ flux to the atmosphere	mol/m ³	daily or monthly	> 2 years	1	M
Ebullition of CH ₄	mol/(m ² s)	daily or monthly	> 2 years	2	O
Diffusive CH ₄ flux	mol/(m ² s)	daily or monthly	> 2 years	2	O
CH ₄ concentration (profiles)	mol/m ³	daily or monthly	> 2 years	2	M
Oxygen concentration (profiles)	mol/m ³	daily or monthly	> 2 years	3	O
C _{labile} (labile carbon density)	mol/m ³	daily or monthly	> 2 years	4	O
CO ₂ concentration (profiles)	mol/m ³	daily or monthly	> 2 years	4	O
Total CO ₂ flux to the atmosphere	mol/m ³	daily or monthly	> 2 years	4	O



Thank you!



Заключение

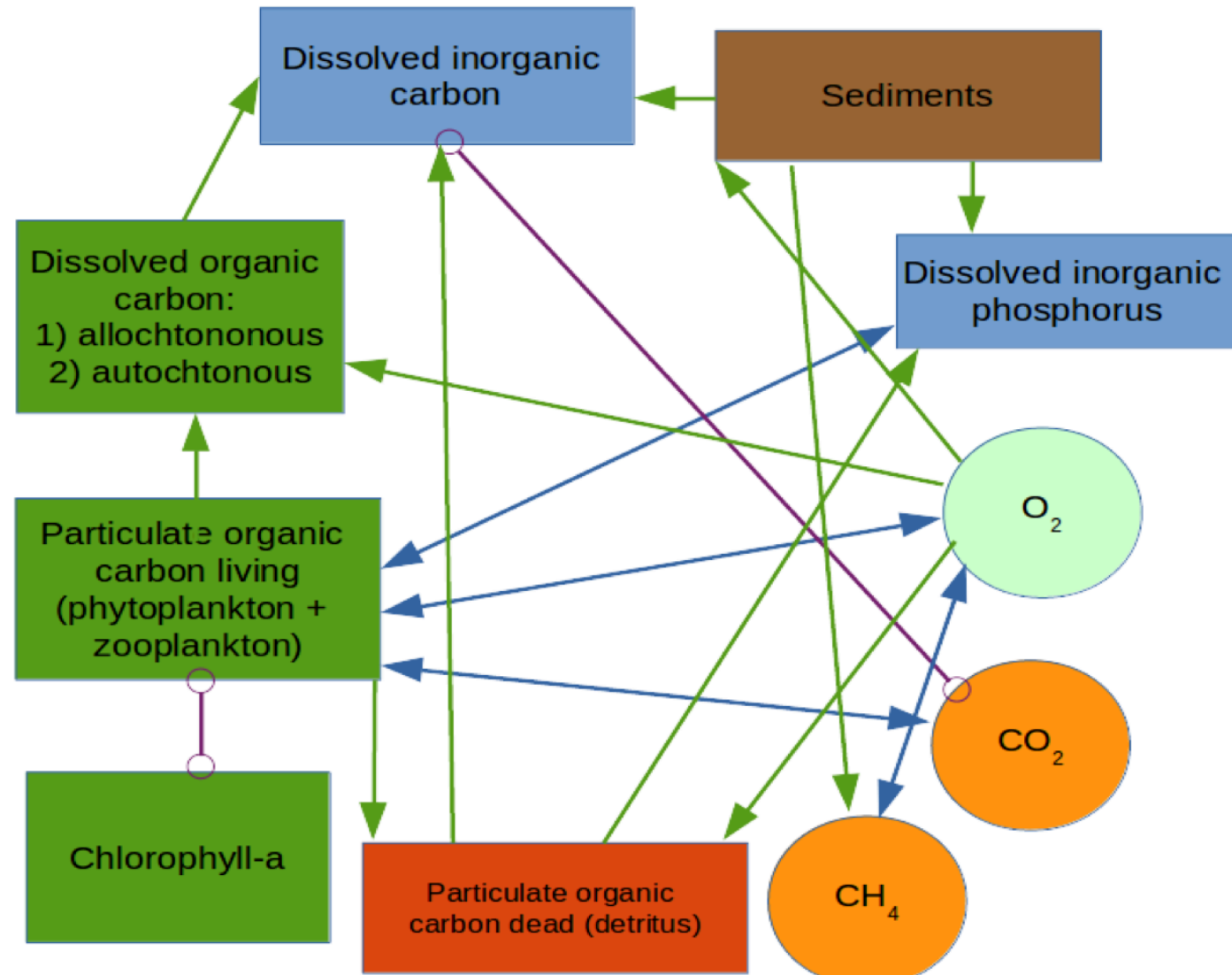
- Mixing in thermocline: existent turbulence closures do not properly reproduce metalimnetic mixing, calibrated background diffusivities are used
- Internal waves are not represented in most 1D models
- Standard 1D model formulations do not reproduce bottom boundary layer
- The physics of saline lakes is understudied
- There is no alternative for Monin-Obukhov similarity for small lakes or lakes with surrounding bluff topography
- Proper understanding and parameterization schemes of interactions between atmosphere, surface waves and currents are missing
- Feedbacks of biological processes on physics (via water turbidity) is lacking in most models



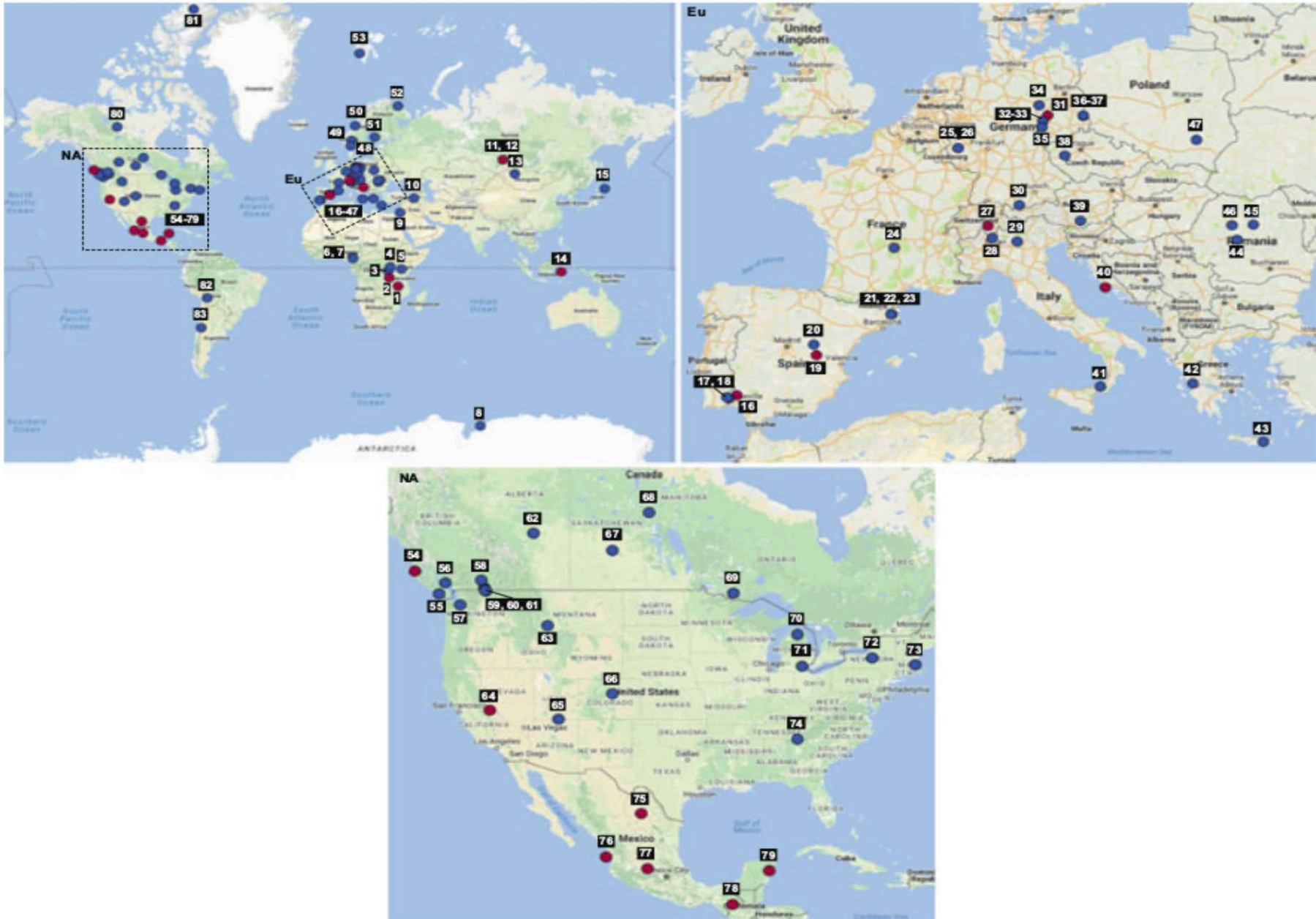
Biogeochemical interactions in the model

(Stepanenko et al., FAC, 2020)

- Photosynthesis, respiration and BOD are empirical functions of temperature, Chl-a and phosphorus
- Oxygen uptake by sediments (SOD) is controlled by O_2 concentration and temperature (Walker and Snodgrass, 1986)
- Methane production $\propto P_0 q_{10}^{T-T_0}$, P_0 is calibrated (Stepanenko et al., 2011)
- Methane oxidation follows Michaelis-Menthen equation



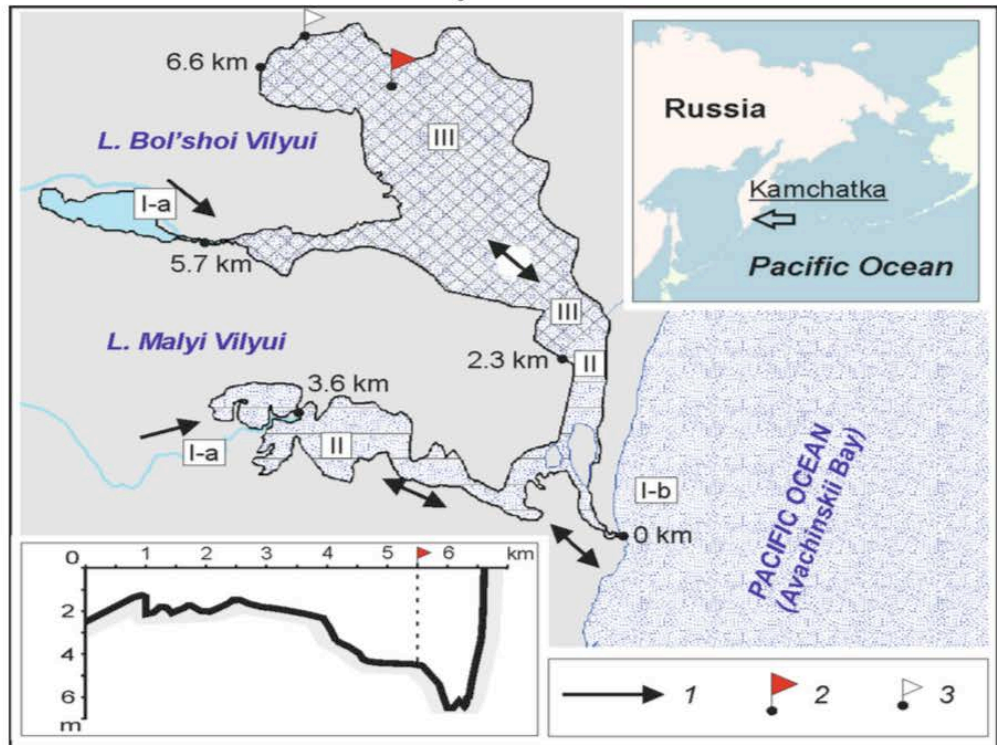
Meromictic lakes (Zadereev et al., 2017)



Temperature maximum in Bol'shoi Vilyui Lake

Measurement campaign, July 2015 (Stepanenko et al., 2018, Env.Res.Lett.)

Bol'shoi Vilyui Lake

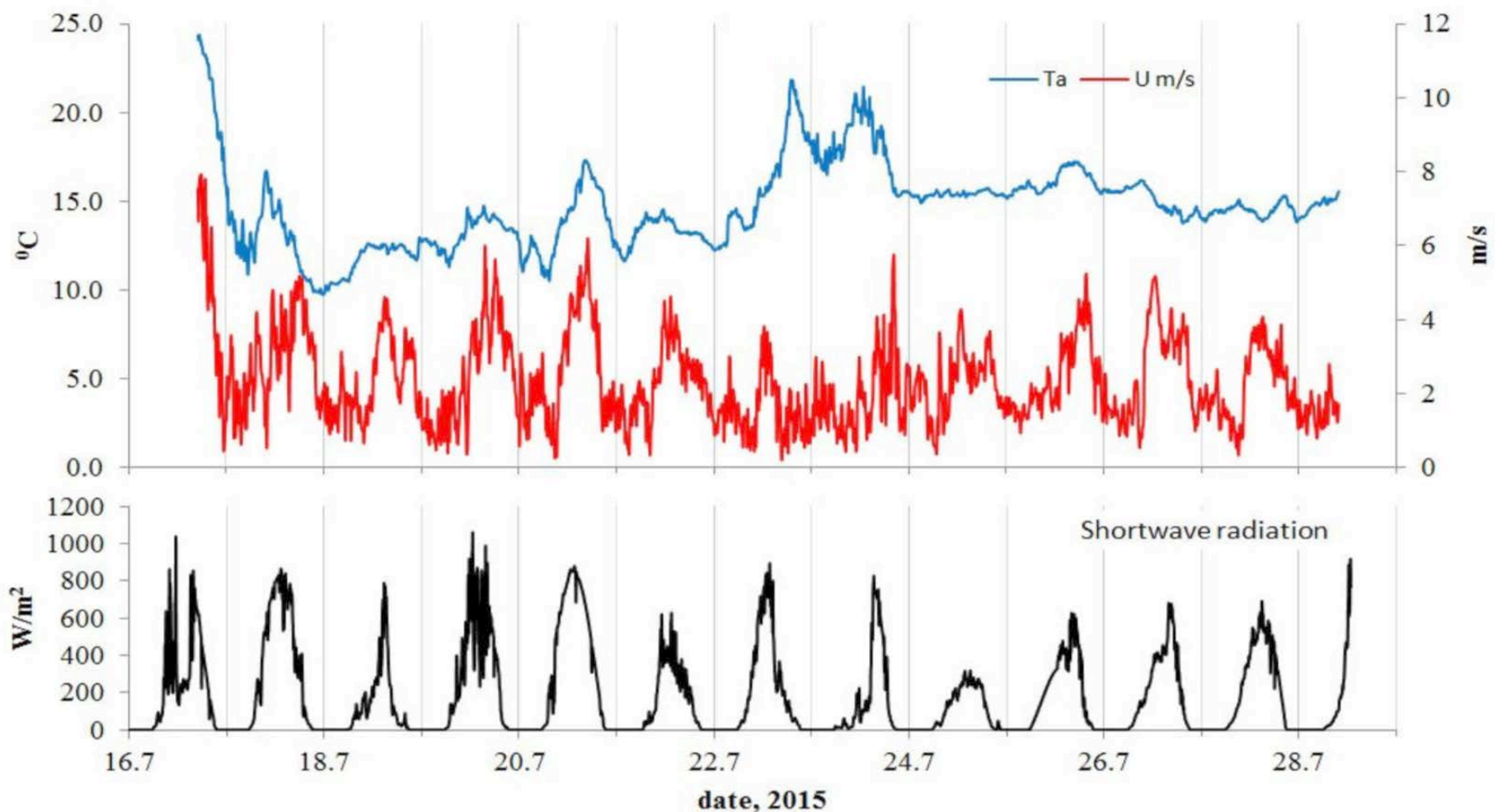


Measurement raft



- Conventional meteorology (Davis Instruments) and radiation fluxes (Kipp & Zonen) at the on-shore station
- Eddy covariance for sensible heat, momentum and CH₄ fluxes, thermistor string on the raft

Meteorology

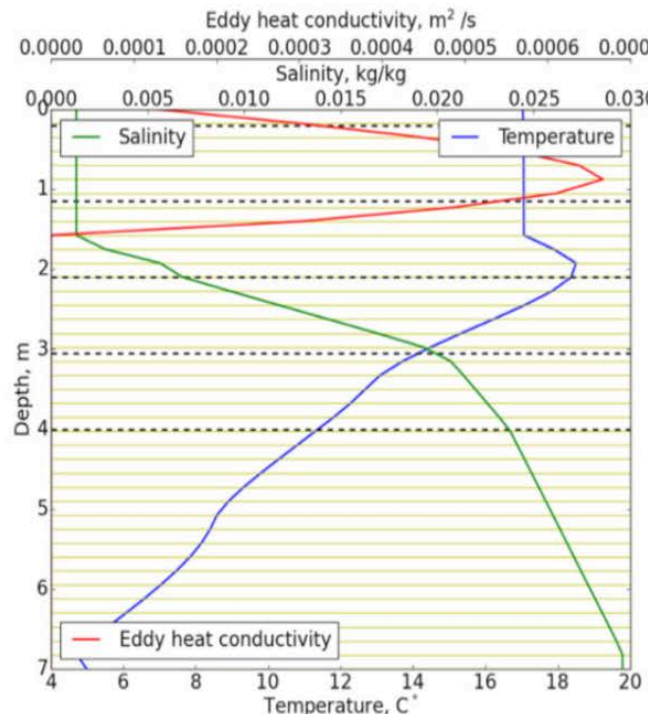
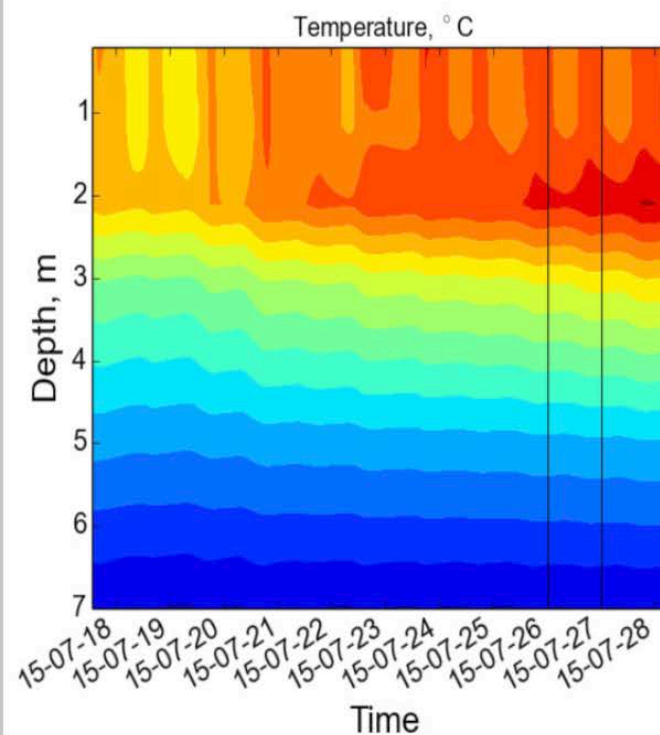


- high shortwave radiation flux due to clear-sky conditions
- diurnal wind cycle with daytime maximum

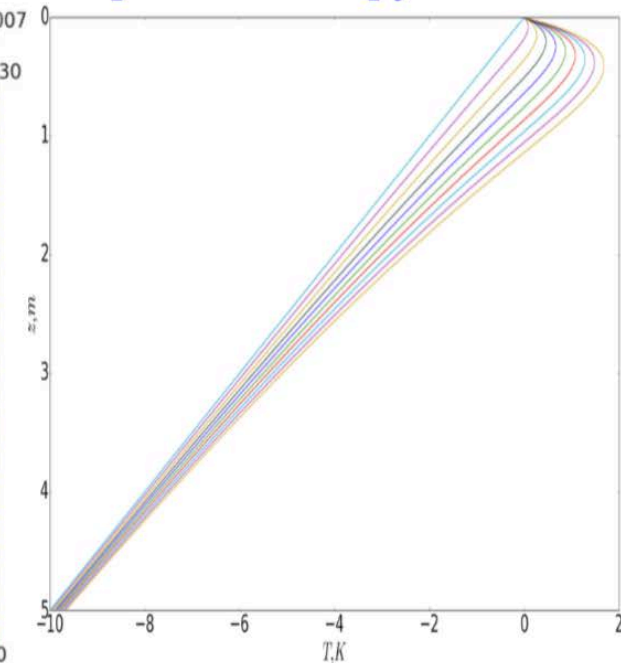
Temperature maximum in Bol'shoi Vilyui Lake

Model results (Stepanenko et al., 2018, Env.Res.Lett.)

Temperature and salinity profiles, modelled



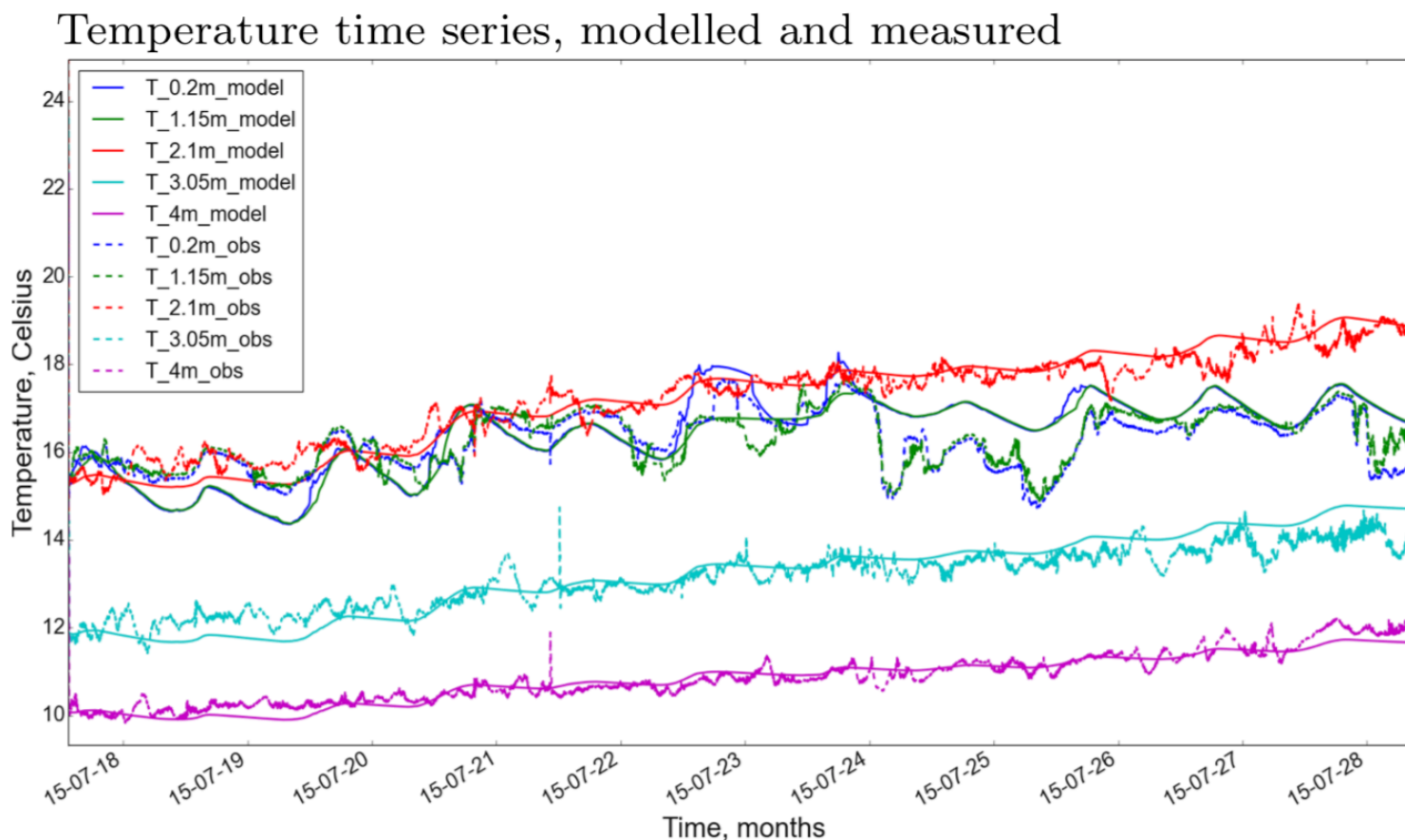
Analytical solution for temperature in pycnocline



- The lake is characterized by profound salinity increase below the freshwater mixed layer, suppressing turbulence and preventing convection at unstable temperature stratification
- Clear-sky conditions favoured radiation heating below the mixed layer

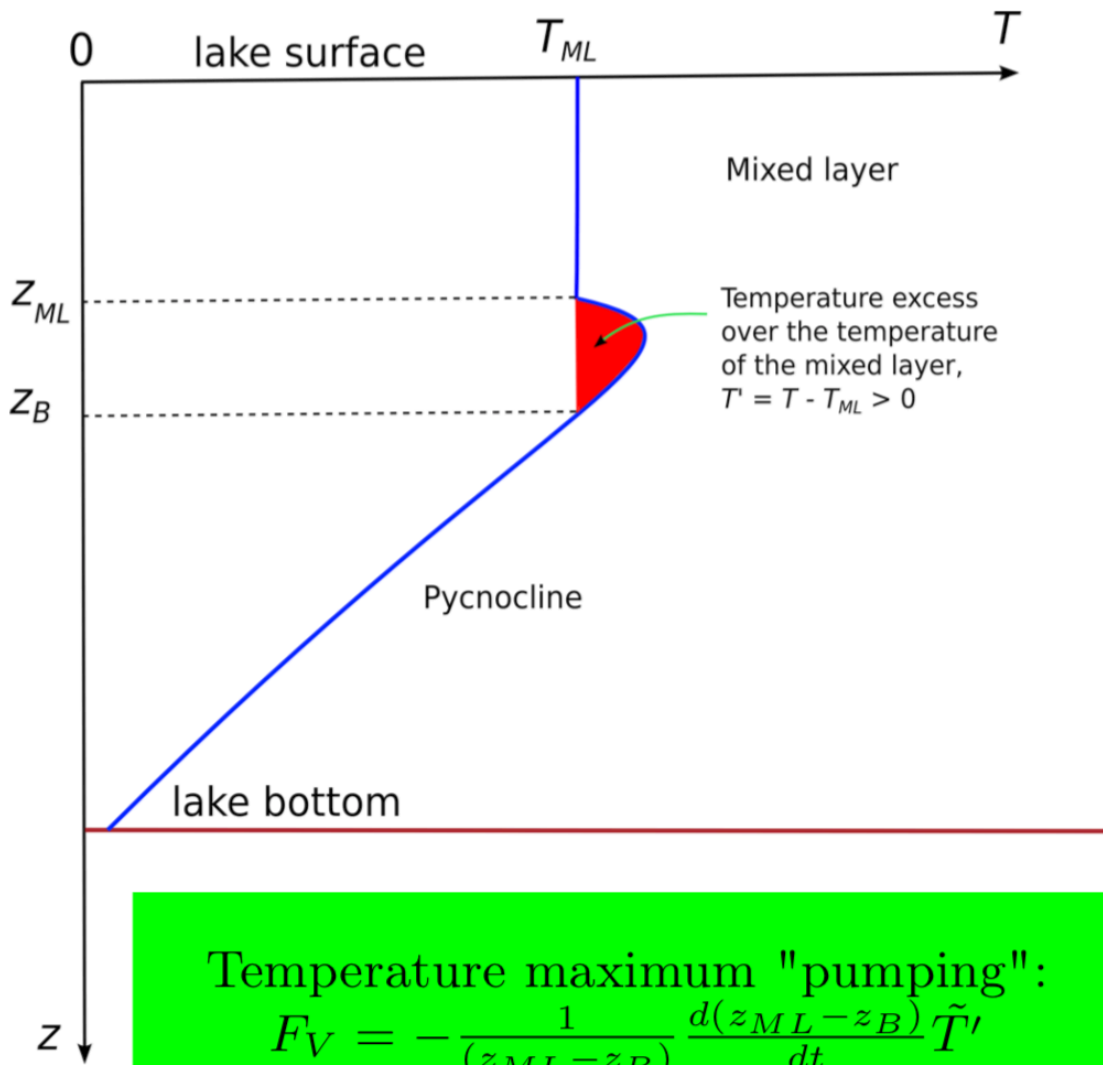
Temperature maximum in Bol'shoi Vilyui Lake

Model verification (Stepanenko et al., 2018, Env.Res.Lett.)



- The model satisfactorily reproduces the measured temperature with $r = 0.64 - 0.95$ and RMSE 0.19-0.71°C
- No calibration has been performed (except for extinction coefficient that has been slightly changed from the observed value)

Heat balance of temperature maximum



Temperature maximum "pumping":

$$F_V = -\frac{1}{(z_{ML} - z_B)} \frac{d(z_{ML} - z_B)}{dt} \tilde{T}'$$

Caused by diurnal cycles of mixed-layer depth (wind speed) and temperature maximum itself

Mean temperature excess over the mixed-layer temperature is a sum of heat balance terms:

Physical mechanism	Contribution to maximum, K
Radiation absorption	+1.9
Mixed-layer temperature dynamics	≈ 0
Vertical temperature diffusion	-1.6
Heat sink to sediments	-0.6
Temperature maximum "pumping"	+0.7
Resulting temperature maximum	+0.5

Summer temperature maximum in meromictic lakes

Lake, location, reference	Depth, m, and magnitude of salinity jump, %	Extinction coefficient, m^{-1}	Temperature maximum depth, m
Shira, Siberia	6-8 m/2-6%	no data	NO
Shunet, Siberia	4.5 m/15%	no data	NO
Cueva de la Mora pit lake, Spain	4.5 m/no data	no data	NO
La Cruz, Spain	10 m/no data	0.35	NO
Sasykkul, Pamir	<2 m/25%	≈1	2
Lake Medve (Bear), Transylvania	0.5 m/200%	no data	1.5
Hot Lake, Washington	0.5-1 m/20%	≈1	1-2
Bolshoi Vilyui, Kamchatka	1.5 m/20%	0.57	≈2



Conclusions on temperature maximum

Conditions favouring summertime temperature maximum:

- small mixed-layer depth; the rough condition on depth, depending on water turbidity, is < 2 m;
- the water in the mixed-layer is not turbid;
- strong salinity gradient in chemocline enough to prevent double diffusion;
- diurnal wind speed cycle with daytime maximum;
- cloudless weather.

In fall, temperature maximum if found in e.g. Fayetteville Green Lake (Brunskill and Ludlam 1969), Aral Sea (Izhitskiy et al 2016), ...

Should we care of temperature maximum? Temperature maximum may overlap with chlorophyll maximum position thus affecting lake primary production through dependence of photosynthesis on temperature? (Eppley, 1972, Quiros, 1988, Kishi et al., 2007)

Saline Lake Uvs (Mongolia)



- largest lake in Mongolia, with surface area 3350 km²
- maximal lake depth 22 m
- Secchi depth 3.8-5.7 m in central part (Horn et al., 2016)
- salinity is decreasing, from 18‰(1930-s) to 14‰(2000)
- strongly continental climate (July 20°C, January -32°C) with small precipitation

Effects of salinity in LAKE model

Salinity in water

- equation of state includes salinity
- freezing point depends on salinity
- release/uptake of salts during ice melting/freezing

Salinity in ice

- ice has pores filled by brine
- porosity at the ice bottom depends on the speed of advancing the ice-water margin
- ice thermal conductivity and specific heat are modified
- thermodynamic constrain $T_{ice} = T_{fr}(s_{pores})$
- freezing/melting of brine in pores affects temperature
- simple parameterization for brine percolation



Sea ice core

Credit: Ken Golden, NSF

Data and model setup

Model parameters:

- initial homogeneous salinity 17‰
- simulation period 1979-2015
- vertical resolution 20 layers
- timestep 20-30 s

Forcing data: ERA-Interim reanalysis

Model experiments:

- "FrWat+FrIce" – fresh water and fresh ice
- "SalWat+FrIce" – saline water and fresh ice
- "SalWat+SalIce" – saline water and saline ice

Validation data:

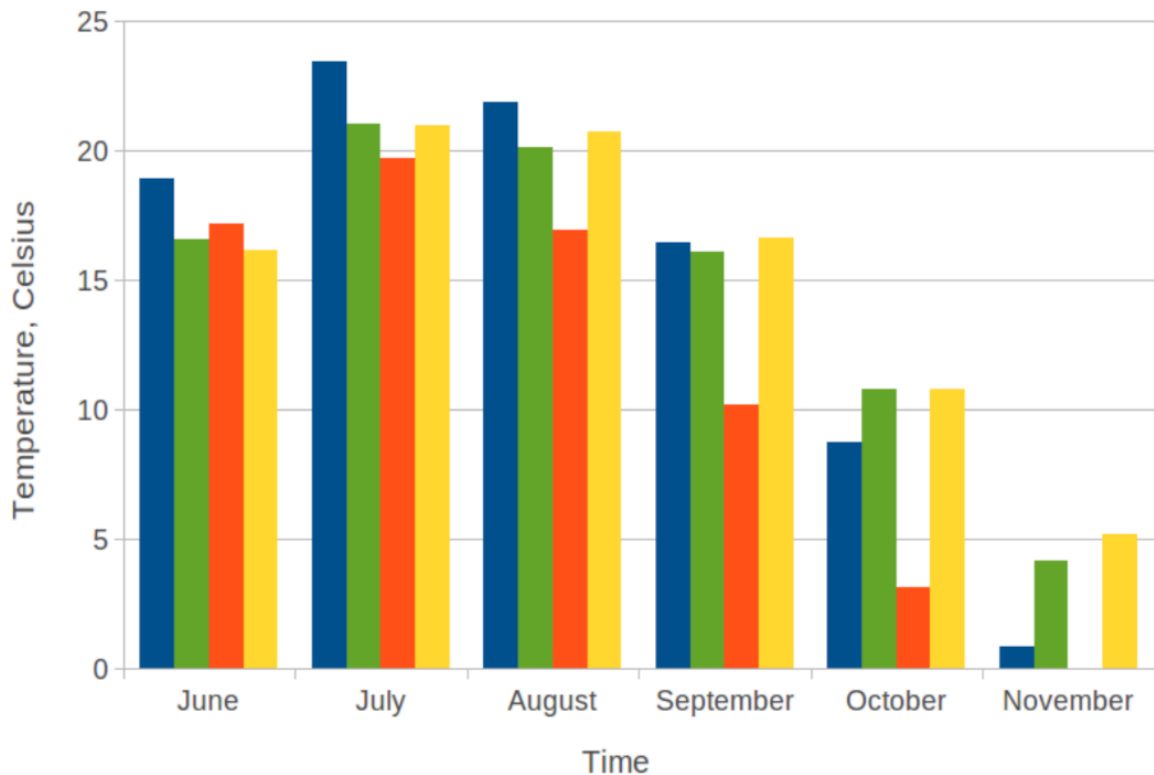
- near-shore water temperature – hydrological station Davst
- mean surface water temperature – MODIS
- ice-on and ice-off dates – MODIS, MIRAS



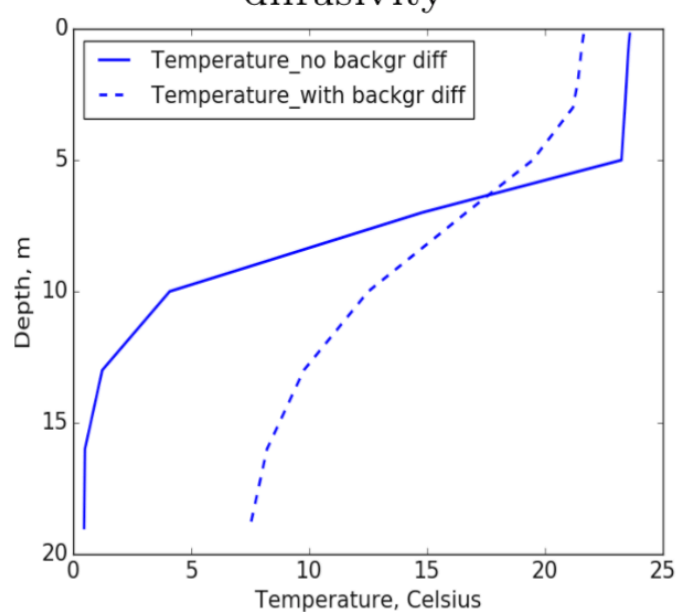
Mesoscale cyclone over Uvs Lake,
27 Nov 2016

Monthly surface temperature

Averaged over 2001-2015



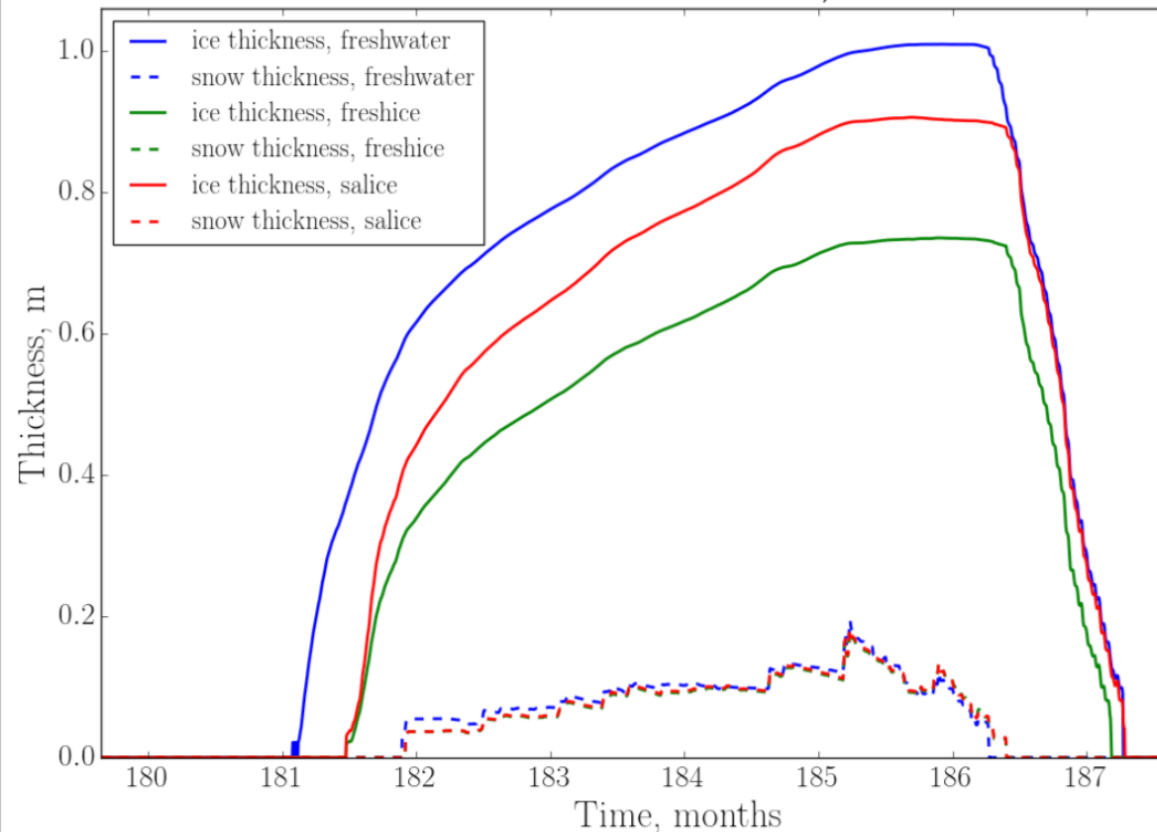
Temperature in Uvs, July 1979,
with and without background
diffusivity



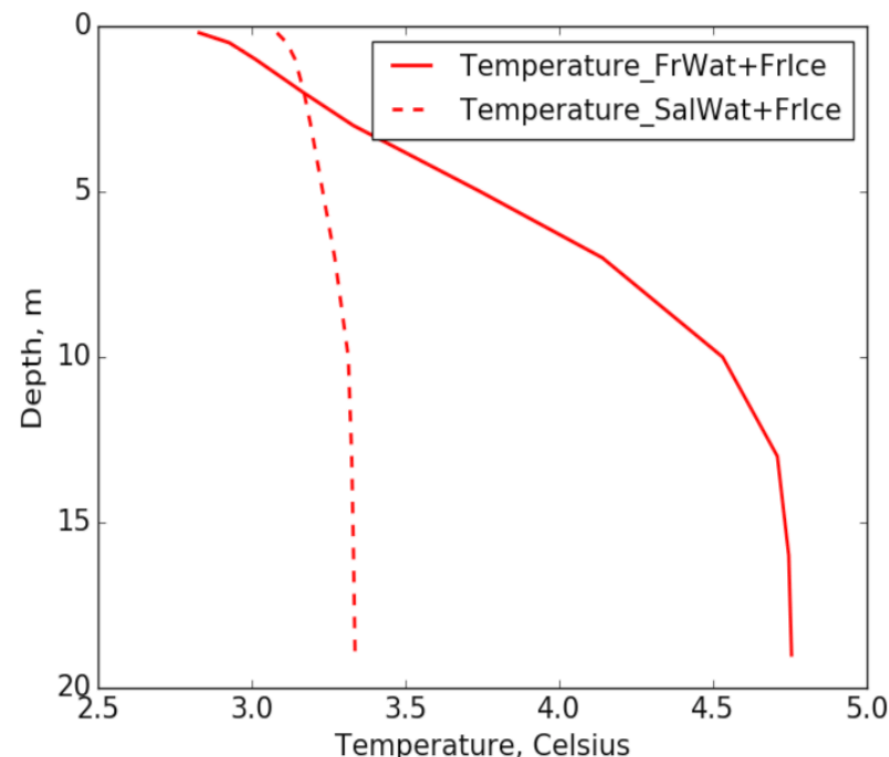
- $k - \epsilon$ model without background diffusivity (blue) produces shallow mixed layer (~ 5 m), overheating it in summer and overcooling it in autumn
- introducing and calibrating background diffusivity by Hondzo and Stefan (1993) largely eliminates this temperature error (green)

Ice and snow thickness

Ice and snow thickness modeled, 1993-1994



Temperature in Uvs, Nov 1981,
fresh and saline water



- Saline ice grows faster compared to fresh ice because of porosity (ice bottom porosity ~ 0.25)

- Fresh lake freezes earlier, because of higher freezing point and ceasing convection after surface temperature falling below 4°C

Ice dates and ice thickness

Ice-on and ice-off dates

Model experiment	Ice-off dates			Ice-on dates		
	FrWat + FrIce	SalWat + FrIce	SalWat + SalIce	FrWat + FrIce	SalWat + FrIce	SalWat + SalIce
Mean deviation (days)	3.3	-0.2	3.1	-16.7	-0.1	-1.7
RMSE (days)	6.1	4.9	5.9	18	4.8	6.6

Mean maximal ice thickness

Model experiment	SalWat + FrIce	SalWat + SalIce	Observations
Mean maximal ice thickness, m	0.77	0.97	0.98

Results may be improved, because:

- radiation properties of ice and snow are kept constant in the model, whereas they vary with time
- fractional ice cover is not taken into account

Conclusions on ice regime of saline lakes

- the new LAKE 2.1 version of the model includes lake ice salinity
- to simulate correct ice-on and ice-off dates "saline water + fresh ice" approximation delivers acceptable results for Uvs Lake → implications to lake parameterization in numerical weather forecast
- if ice thickness is important, salinity dynamics in ice should be taken into account
- further improvement of the snow-ice scheme should focus on fractional ice cover effects and evolution of radiation properties of ice and snow

LAKE model website

LAKE model

<http://tesla.parallel.ru/Viktor/LAKE/-/wikis/LAKE-model>

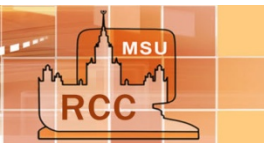


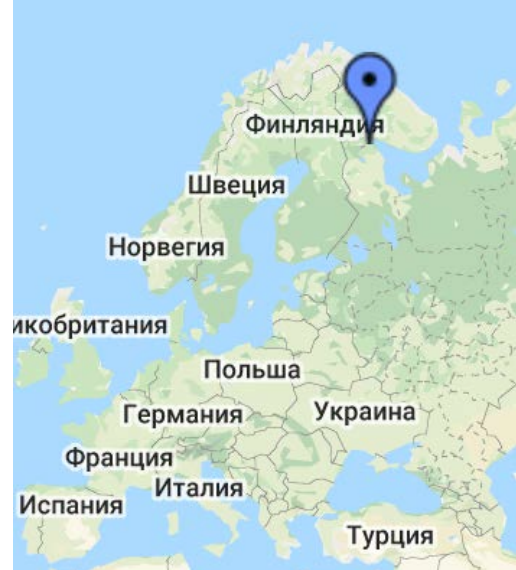
LAKE is an extended one-dimensional model of thermodynamic, hydrodynamic and biogeochemical processes in the water basin and the bottom sediments (Stepanenko and Lykosov 2005, Stepanenko et al. 2011). The model simulates vertical heat transfer taking into account the penetration of short-wave radiation in water layers (Heiskanen et al., 2015), ice, snow and bottom sediments. The model allows for the evolution of ice layer at the bottom after complete lake freezing in winter. The equations of the model are formulated in terms of quantities averaged over the horizontal section a water body, which leads to an explicit account of the exchange of momentum, heat, and dissolved gases between water and the inclined bottom. In the water column, $k - \epsilon$ parametrization of turbulence is applied. The equations of motion take into account the barotropic (Stepanenko et al., 2016) and baroclinic pressure gradient (Степаненко, 2018). In ice and snow, a coupled transport of heat and liquid water is reproduced (Volodina et al. 2000; Stepanenko et al., 2019). In bottom sediments, water phase changes are simulated. The model also describes vertical diffusion of dissolved gases (CO_2 , CH_4 , O_2), as well as their bubble transfer, methane oxidation, photosynthesis and processes of oxygen consumption. Parameterization of methane production in sediments is included (Stepanenko et al. 2011), and for the case of thermokarst lakes, an original formulation for the methane production near the lower boundary of "talik" is implemented. Model was tested in respect to thermal and ice regime at a number reservoirs in contrasting climate conditions, specifically, within the LakeMIP project (Lake Model Intercomparison Project, Stepanenko et al., 2010; Stepanenko et al., 2013; Stepanenko et al., 2014; Thiery et al., 2014).

The current **version** of the model is 2.3

The complete **model archive** with sample input data:

- [LAKE2.0.zip](#)
- [LAKE2.1.zip](#) (salinity dynamics in ice cover is added)
- [LAKE2.2.zip](#) (input/output of control point added, minor bugs fixed)
- [LAKE2.3.zip](#) (commit `7d016e79` in gitlab repository, which is updated by testing at GNU Fortran 9.3.0 compiler; the model is adapted to simulate artificial reservoirs with high throughflow and water level variations; a model configuration for simulating the vertical structure of river flow is added)
- [LAKE2.4.zip](#) (commit `f29fb387` in repository; bugs related to $k - \epsilon$ model fixed, new b.c. options for $k - \epsilon$, Cuette-Poiseuille flow setup and turbulence closure added, methane production parameters are set specific for each sediment column, new output options)





White Sea lake experiment-1

(Barskov et al., 2019)

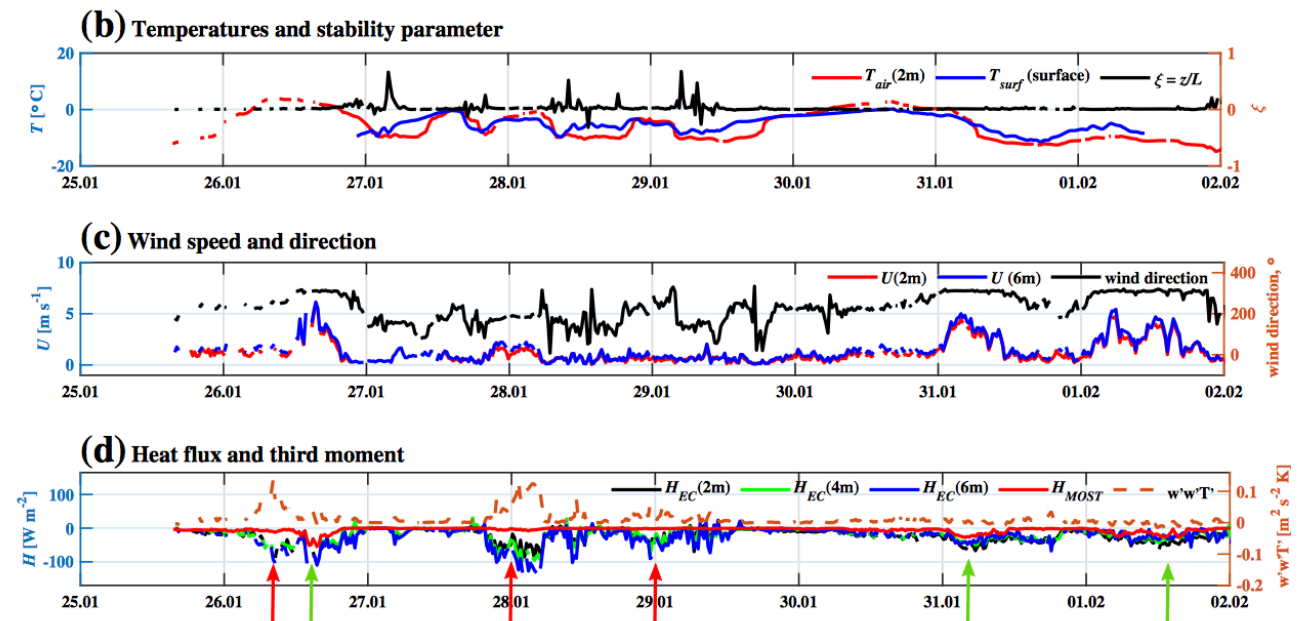
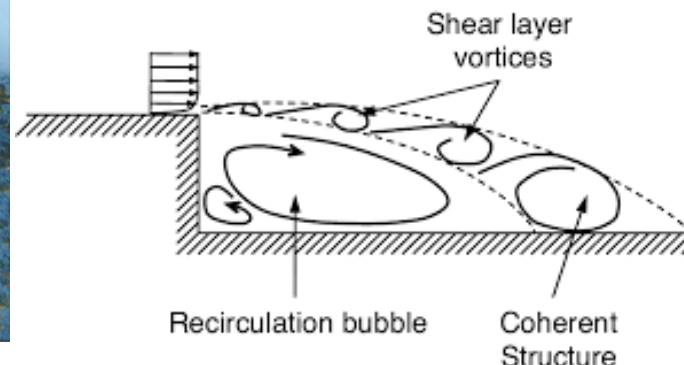


Fig. 1 The temperature profile up to 1 km (a), air temperature at 2 m, temperature at the surface and stability parameter ξ (b), wind speed and direction (c), and time series of sensible heat flux, measured directly (H_{EC}) at 2, 4, and 6 m, calculated by MOST H_{MOST} , and third moment $w'w'T'$ (d). Dates are from 25 January to 2 February

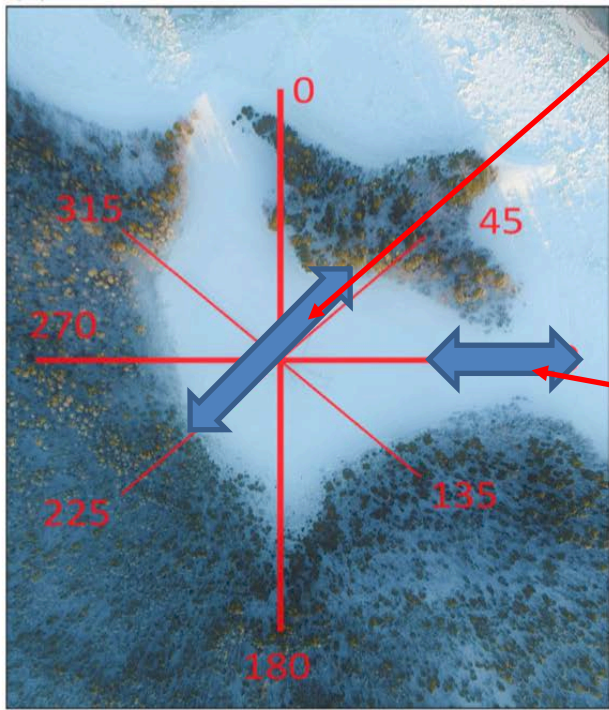


Third moments, e.g. $\overline{w'w'T'}$ are indicative of coherent turbulent structures, such as vortices after backward step.

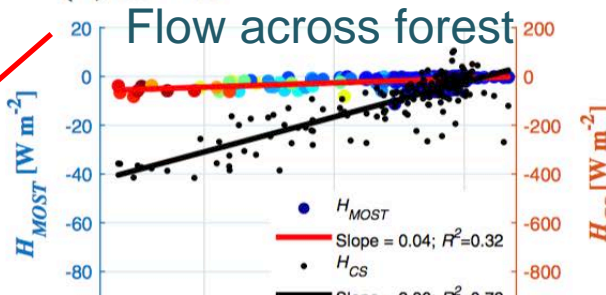
White Sea lake experiment-2

(Barskov et al., 2019)

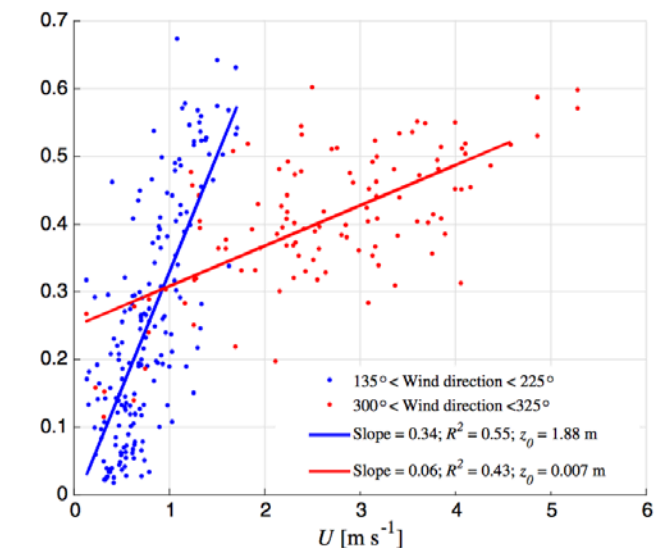
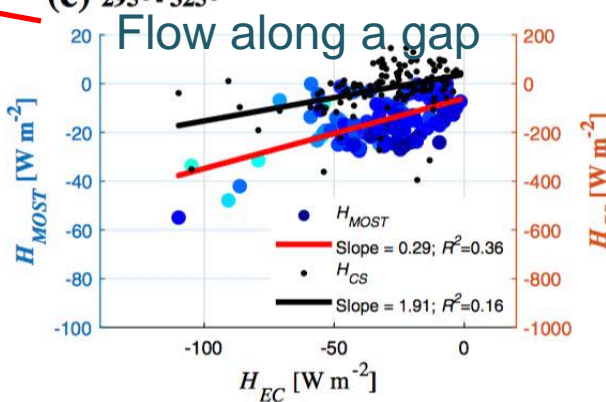
(a)



(b) 135° - 225°



(c) 295° - 325°

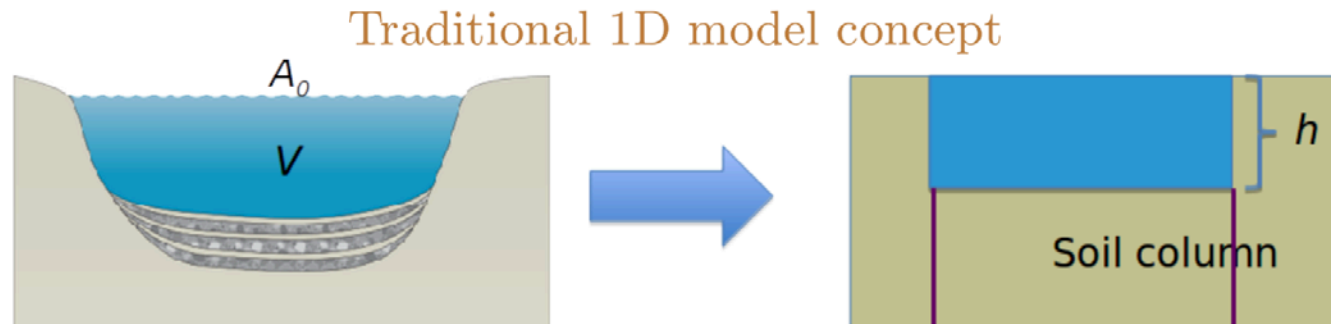


$$H_{CS} = -C_p \rho \overline{w' T'} = -C_P \rho \frac{\overline{w' w' T'}}{S_w (w'^2)^{\frac{1}{2}}}$$

Fig. 3 Lake with wind-directions diagram (a), scatter plot H_{MOS} and H_{CS} versus H_{EC} when the flow is from the vast forest (b), and from the northern gap (c). Colour scale is given for the third moment $\overline{w' w' T'}$

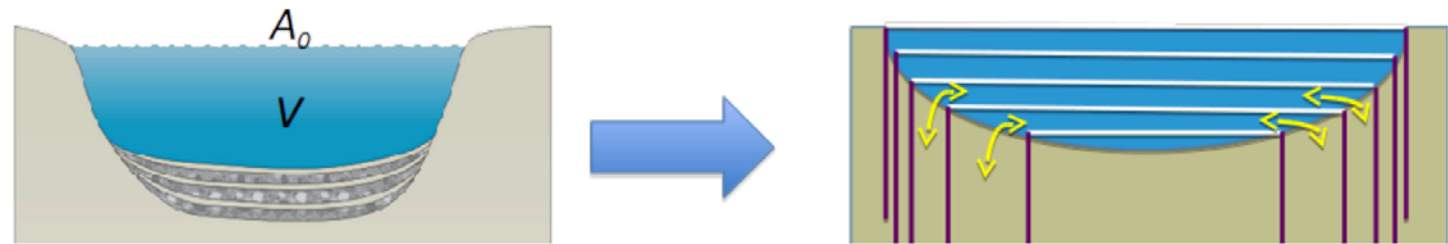
Monin-Obukhov theory fails to simulate observed fluxes for small fetches and bluff topography

$1D^+$ framework



$1D^+$ model concept

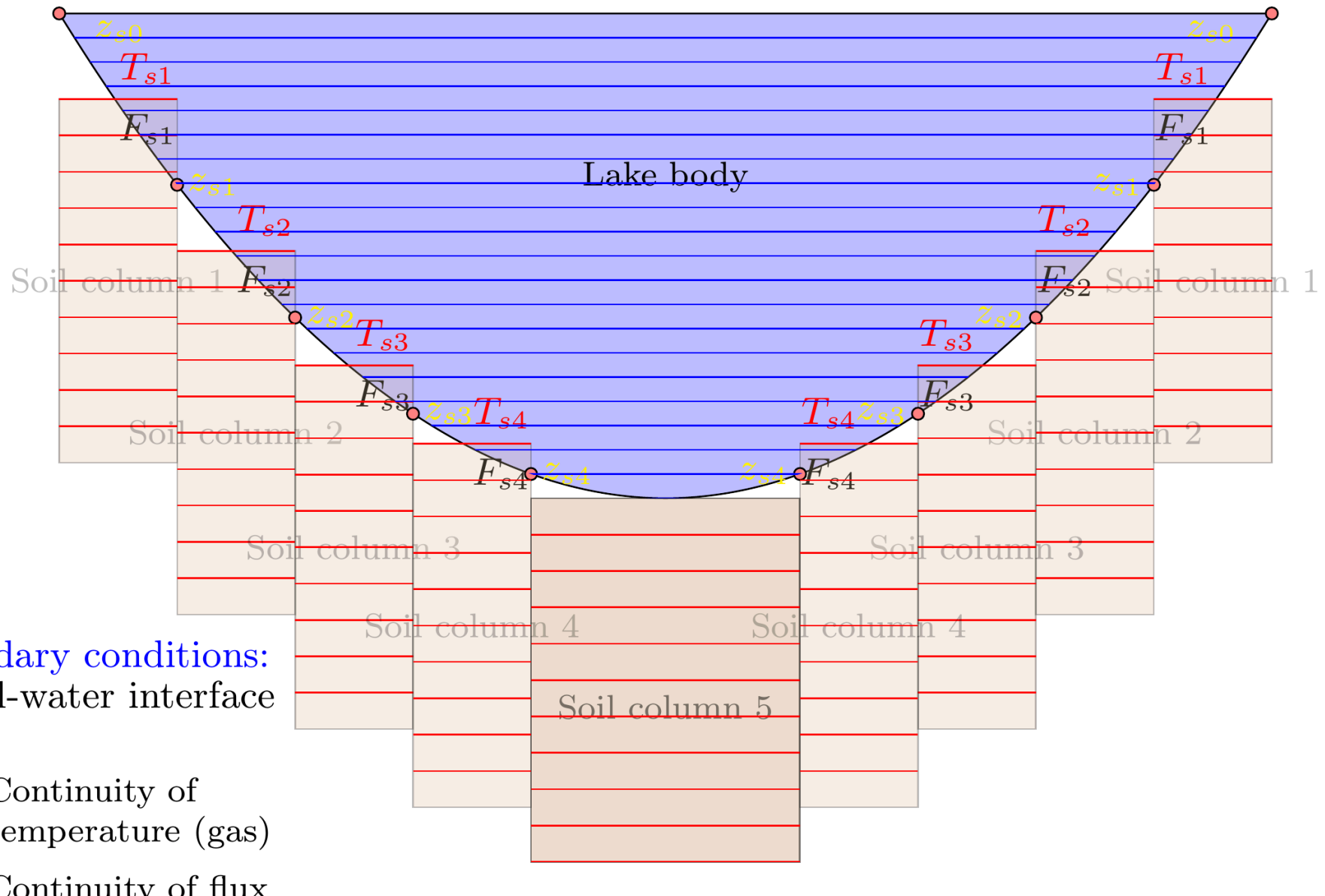
- $1D^+$ model includes friction, heat and mass exchange at the lateral boundaries
- Heat, moisture and gas transfer are solved for each soil column independently



In $1D^+$ model horizontally averaged quantity f obeys the equation:

$$\frac{\partial f}{\partial t} = \frac{1}{A} \frac{\partial}{\partial z} [A k_f \frac{\partial f}{\partial z} + F(z, t, f, A)] + H_f \frac{1}{A} \frac{dA}{dz}.$$

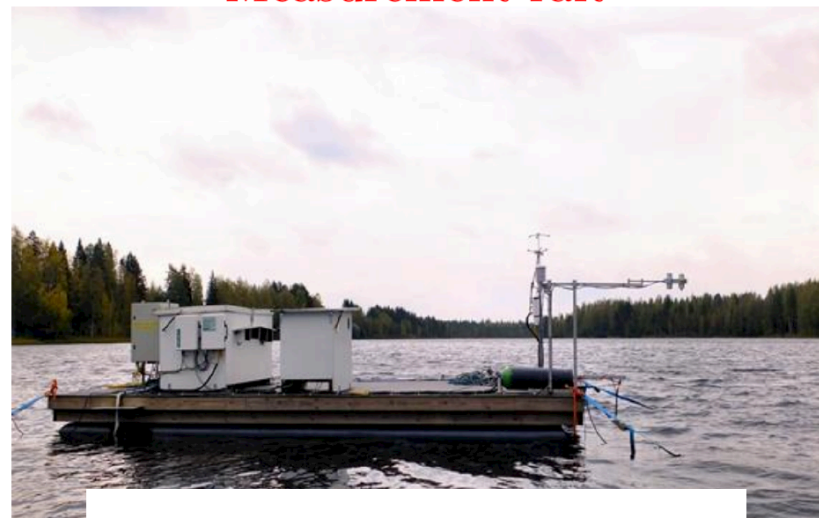
Coupling heat transport in water and soil



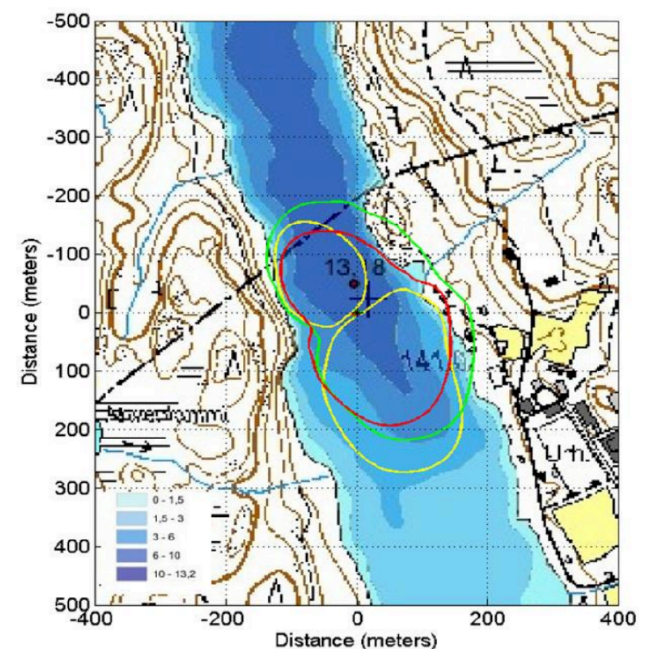
Measurements

- Conducted since 2009 by University of Helsinki
- Ultrasonic anemometer USA-1, Metek GmbH
- Enclosed-path infrared gas analyzers, LI-7200, LI-COR Inc.
- Four-way net radiometer (CNR-1)
- relative humidity at the height of 1.5 m (MP102H-530300, Rotronic AG)
- thermistor string of 16 Pt100 resistance thermometers (depths 0.2, 0.5, 1.0, 1.5, 2.0, 2.5, 3.0, 3.5, 4.0, 4.5, 5.0, 6.0, 7.0, 8.0, 10.0 and 12.0 m)
- Turbulent fluxes were calculated from 10 Hz raw data by EddyUH software

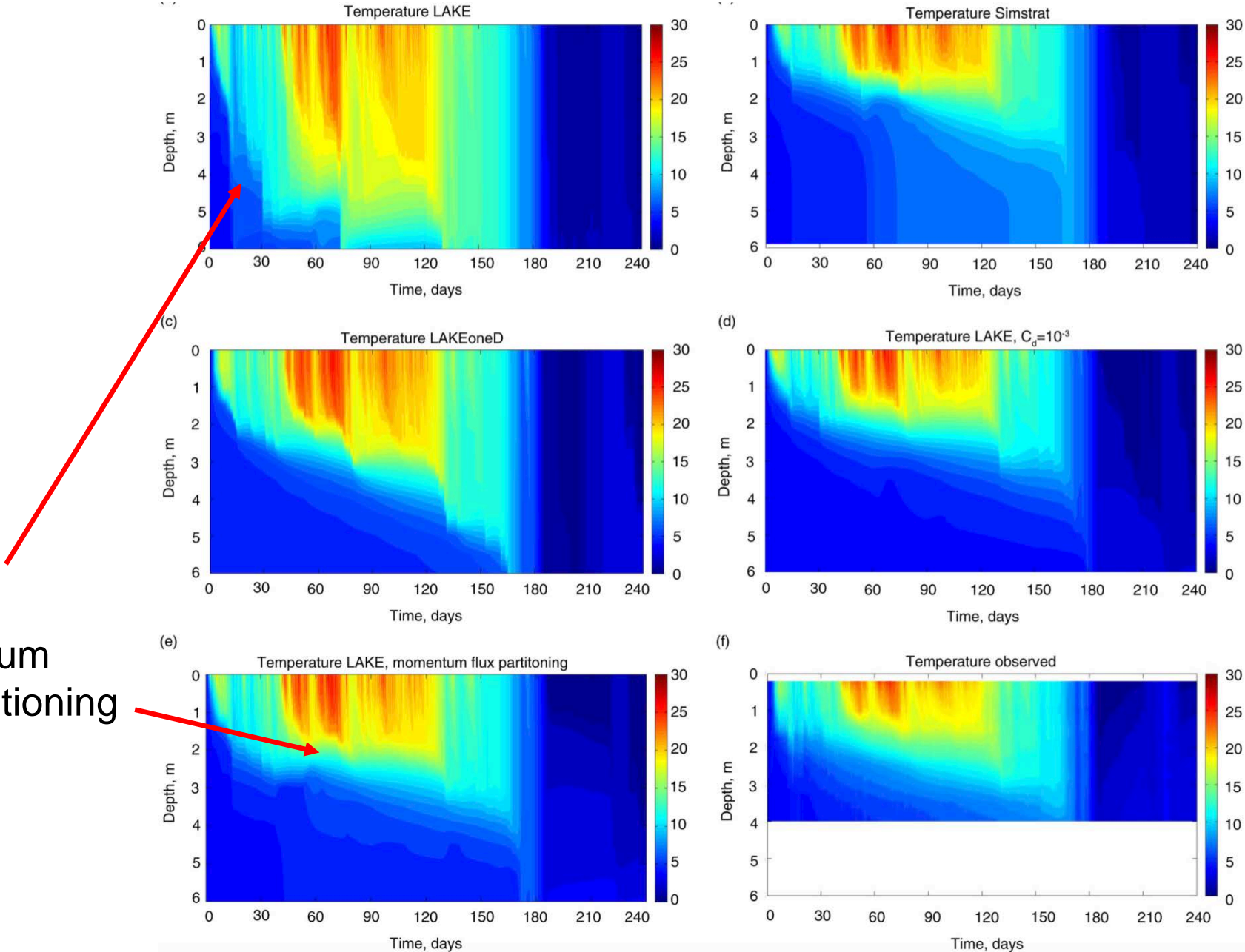
Measurement raft



Footprint of the raft measurements



Valkea-Kotinen Lake: stratification



Effect of
momentum
flux partitioning

Measurement data

- conventional meteorology from nearby Mozhayskoe station, corrected using empirical relations to on-lake conditions
- radiation fluxes from Zvenigorod station (IAP RAS)
- discharge data from a dam
- string of temperature loggers at the deep part (V) of reservoir
- whole-lake surveys of water temperature, dissolved oxygen, methane (headspace method)



Results with Iseo Lake : temperature series

(Stepanenko, Valerio, Pilotti, JAMES, 2020)

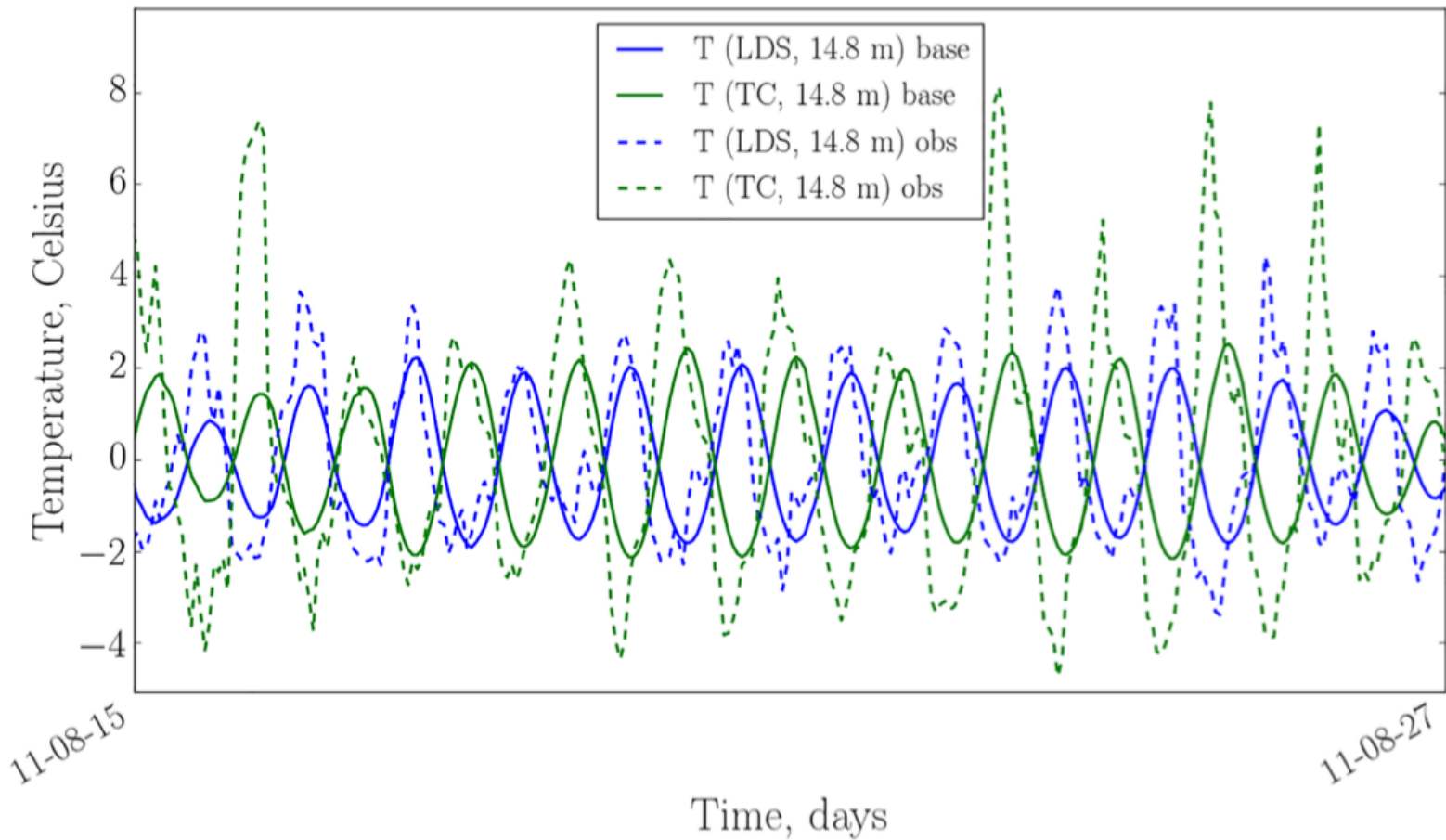


Figure 9. The same as Figure 8 but for TC (14.8 m) and LDS (14.8 m) locations.

Results with Iseo Lake : temperature series

(Stepanenko, Valerio, Pilotti, JAMES, 2020)

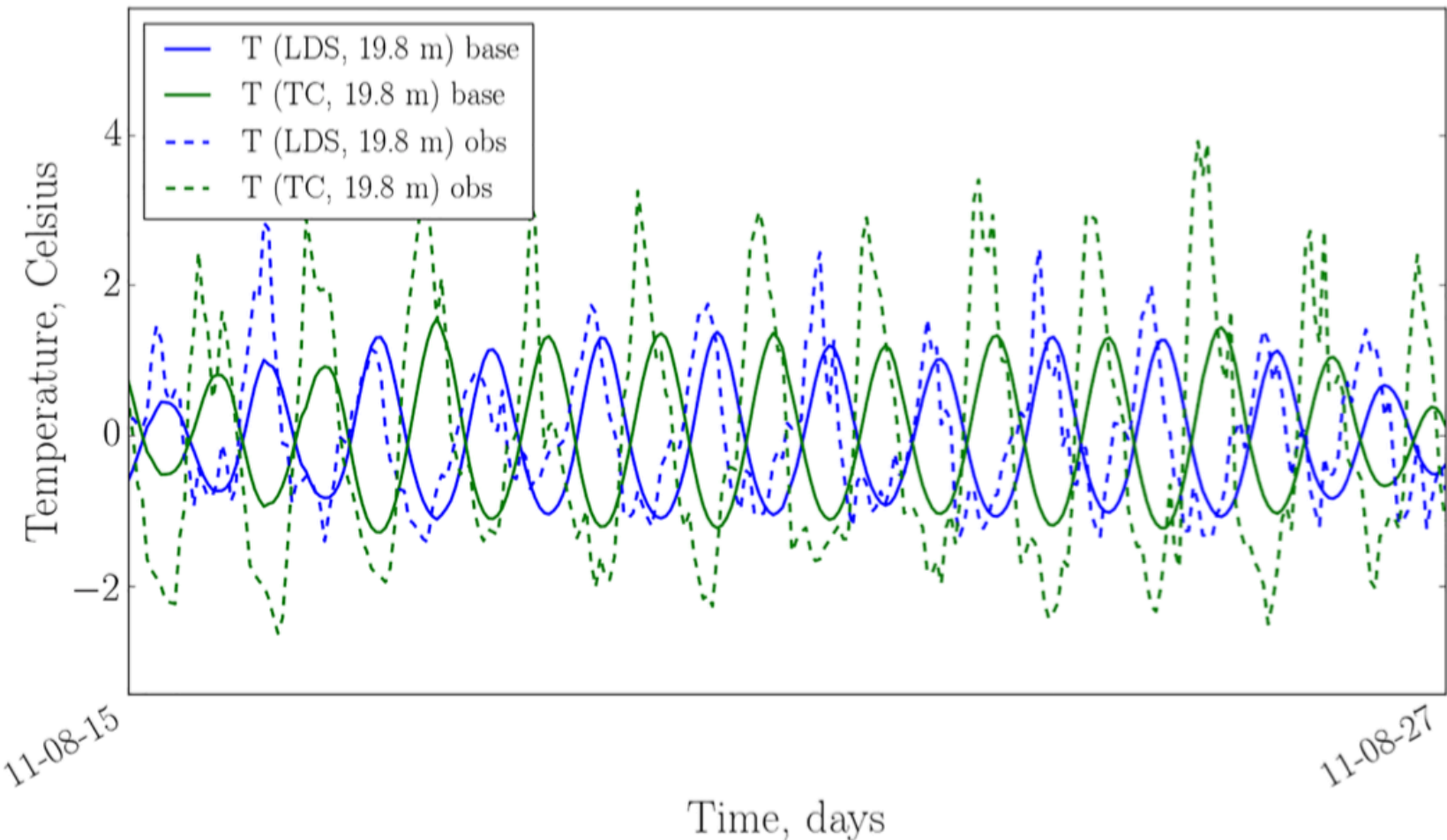
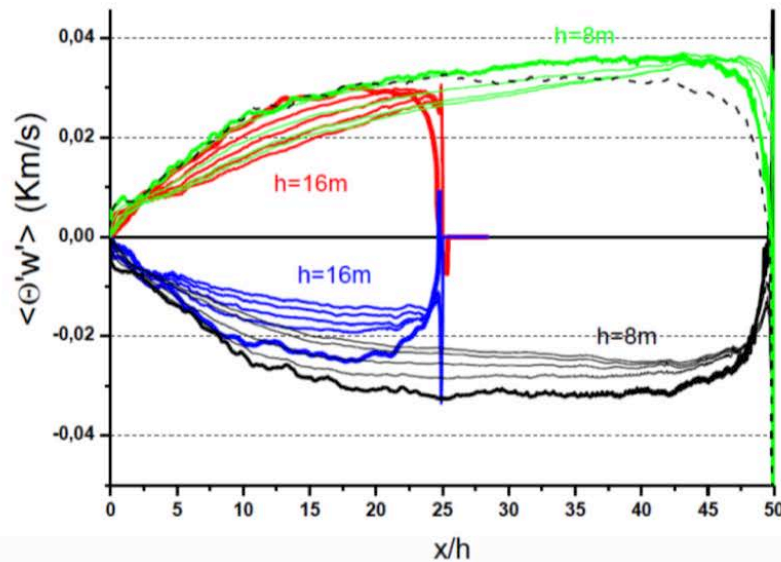
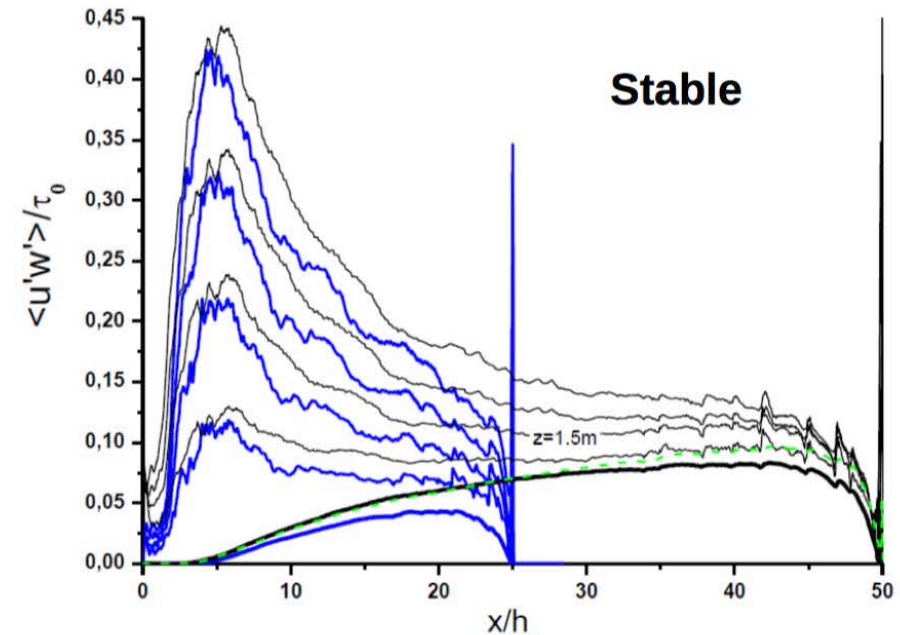
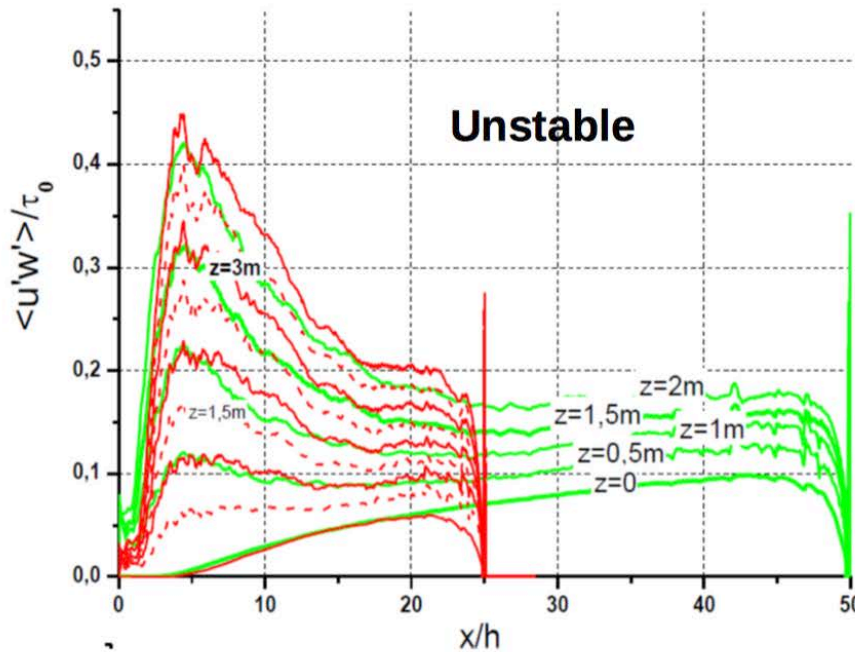


Figure 10. The same as Figure 8 but for TC (19.8 m) and LDS (19.8 m) locations.

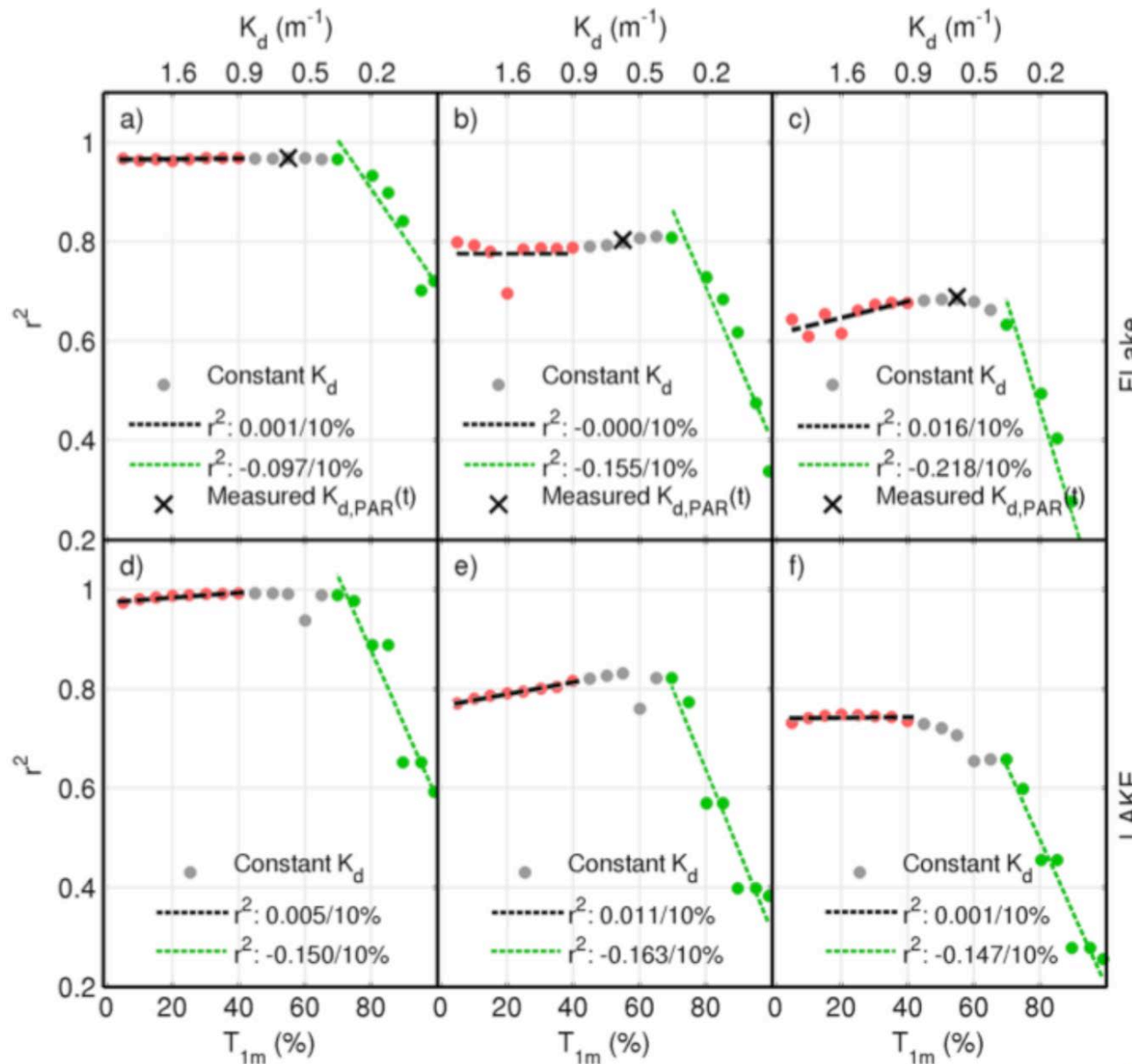
Momentum and heat fluxes at several levels under unstable and stable stratification



Computed (or measured) momentum flux at the height ~ 1.5 m substantially differs from the surface stress, consistent with lake model experiments

Glazunov and Stepanenko, 2015,
Izvestiya, Atmospheric and Oceanic Physics

Kuivajarvi Lake: water turbidity



The lake mixed-layer temperature is sensitive to the extinction coefficient when the characteristic depth of radiation penetration exceeds the depth of the mixed layer, which in turn is due to the wind action and buoyancy flows on the surface.